A project Report on

Use of Thermal Autofrettage for Defence Application

Project Number: ARMREB/ADMB/2021/234

Submitted to

Armament Research Board, DRDO

Department of Mechanical Engineering

Tezpur University, Tezpur-784028,

Assam, India

&

Department of Mechanical Engineering,

Indian Institute of Technology Jammu, Jammu-181221,

J&K India

A project Report on

Use of Thermal Autofrettage for Defence Application

Project Number: ARMREB/ADMB/2021/234

Date of Sanction: 14 June 2021 (Amended on 21 Sep 2021)

Project Start Date: 15 Nov 2021

Project End Date: 25 March 2023

PI:

Dr. Seikh Mustafa Kamal,

Department of Mechanical Engineering,

Tezpur University, Tezpur- 784028, Assam, India

Co-PI:

Dr. Roshan Udaram Patil,

Indian Institute of Technology Jammu,

Jammu- 181221, J&K, India

1. Summary of the Project

Thermal autofrettage is a method that employs a certain temperature difference across the wall thickness of a thick-walled cylinder to cause plastic deformation of the inner wall. Later on, after achieving the desired level of plastic deformation in the cylinder, the applied temperature difference is vanished by cooling it to the room temperature. This action of loading and unloading of a plastically deforming temperature difference induces compressive residual stresses at the inner side of the cylinder and some portion beneath it. The primary objective of the project was to explore the use of thermal autofrettage for strengthening armament gun barrels. The process was considered to investigate for real gun barrel material *i.e.*, ESR steel to be supplied by ARDE, DRDO. An experimental set up was considered to be developed for thermal autofrettage of gun barrel of actual material (ESR) and through detailed experimentation, it was proposed to investigate residual stresses, crack growth and fatigue life and other associated performance parameters. For achieving thermal autofrettage in the gun barrel, it is considered that heat the outer wall using electric heating element and a cold fluid is considered to circulate through its bore to create the desired temperature difference. As the outer wall of the barrel is subjected to heating to reach a certain higher temperature, the thermomechanical properties of the barrel material may change with temperature. Thus, first the temperature dependent thermomechanical properties of the actual gun barrel material (ESR steel) is determined experimentally. Subsequently, using the actual temperature dependent material properties, the thermal autofrettage of gun barrel is simulated in a numerical framework using COMSOL and ABAQUS finite element packages. In this report, the achievements attained so far in line with the proposed objectives are discussed.

2. Introduction

The autofrettage process plays a crucial role in the design of weapon system. The process is employed in gun barrels in order to increase its pressure carrying capacity during firing of projectile as well as to increase its fatigue life. The principle of autofrettage process is based on the generation of beneficial compressive residual stresses at and around the inner surface of a thick-walled cylindrical tube by loading and unloading of a plastically deforming load. The process was originally developed for strengthening gun/canon barrels in the year 1907 by Jacob [1], a French artillery officer. Over the years, the process finds wide range of applications in other industries such as nuclear power plants, space shuttles, submarine hauls, pressure vessels used in oil and chemical industries etc. The commonly practiced autofrettage processes for strengthening gun barrels are hydraulic [2] and swage autofrettage [3]. Recently, the principal investigator of this proposal has developed an alternative autofrettage process called thermal autofrettage [4–8] for cylindrical pressure vessels. The physical principle of the process is described below.

Physical principle of thermal autofrettage:

In thermal autofrettage, the cylinder to be autofrettaged is first subjected to a certain amount of temperature difference across its wall thickness. During the procedure, the outer surface of the cylinder is heated to a temperature which is much below its recrystallization temperature and the inner surface is cooled by flowing some cold fluid through the bore [4, 5]. After achieving the desired level of plastic deformation at the inner layer, the temperature difference is removed, *i.e.*, the cylinder is cooled to room temperature that induces compressive residual stresses at the inner side.

This project intends to explore the feasibility of the new thermal autofrettage method for strengthening gun barrel. In order to achieve the objective of the project, the following scopes of work were identified:

i. To develop an experimental setup for an innovative thermal autofrettage process for gun barrel.
ii. To assess residual stresses, pressure carrying capacity, material properties and microstructural characterization of thermally autofrettaged cylinder/barrel.
iii. To relieve tensile residual stresses in the thermally autofrettage tube.
iv. To measure dimensional changes and bore straightness in the thermally autofrettaged cylinder/barrel.
v. To develop a numerical model for crack propagation in a thermally autofrettaged barrel and to experimentally determine the critical stress intensity factor $K_{IC.}$

In the succeeding sections, the certain milestones achieved towards accomplishing the scopes (i), (ii) and (v) are discussed.

Scope of Work: To develop an experimental setup for an innovative thermal autofrettage process for gun barrels.

Milestones Achieved:

- In order to determine the temperature difference required for thermal autofrettage of an actual gun barrel material, it is important to determine the thermomechanical properties of gun barrel ESR material as a function of temperature. Thus, first, different experiments were conducted to obtain certain parameters which are of interest in view of thermal autofrettage to assess their dependency on temperature.
- An analytical model incorporating the temperature dependent material properties to determine the yield onset temperature difference for ESR barrel.
- Layout design of thermal autofrettage experimental setup for ESR barrel.

3. Experimental Determination of Thermomechanical Properties of Gun Barrel Material

The mechanical properties of gun barrel material at room temperature are presented in Table 1. So far the thermal autofrettage is concerned; the temperature dependent thermomechanical properties are of interest to assess its applicability to ESR gun barrel. This is also important to decide on a suitable experimental set up for the barrel. Therefore, first it was decided to determine the thermomechanical properties of ESR steel (gun barrel material) experimentally.

Table 1 Mechanical properties of gun barrel material at room temperature

Sr. No.	Properties	Value
1	0.2 % Proof Stress (σ_Y)	1050 MPa
2	Young's Modulus of Elasticity (E)	208 GPa
3	J_{IC}	91 kJ/m^2
4	Density (ρ)	7850 kg/m^3
5	Hardness	340-365 BHN
6	Poisson's ratio (v)	0.33

The following thermomechanical properties of ESR steel that influences thermal autofrettage were determined experimentally:

- Coefficient of thermal expansion as a function of temperature
- Yield stress as a function of temperature
- Thermal conductivity as a function of temperature.

Some thermo-mechanical properties (mechanical properties at elevated temperature) of Barrel material were tested in NABL accredited Lab (KCTI, Pune) and some (thermal conductivity and thermal expansion coefficient) are at DRDO Lab (HEMRL, Pune).

3.1 Experimental estimation of coefficient of thermal expansion of ESR steel

The experiment for determining the coefficient of thermal expansion of ESR steel was carried out at High Energy Materials Research Laboratory (HEMRL), Pune, DRDO. The experiments were conducted using thermo-mechanical analyser as shown in Fig. 1. For the thermal expansion coefficient experiments, ESR steel Specimens were prepared as per following ASTM standards: ASTM E831, ASTM D696, ISO 11359. The thermal expansion coefficient of ESR steel were experimentally determined at different temperatures and the results are presented in Table 2.

Fig. 1 Thermo-mechanical Analyser

Table 2 The coefficient of thermal expansion (α) of the ESR steel gun barrel as a function of temperature

Sr. No.	Temp. (°C)	α(x10^{-6}) /°C
1	27	10.30
2	100	10.41
3	200	10.29
4	300	10.64
5	400	11.58
6	500	12.33

The experimental coefficients of thermal expansion of ESR steel presented in Table 2 are plotted in Fig. 2 as a function of temperature. By fitting the experimental data points, it is seen that the coefficient of thermal expansion of ESR steel increases with increase in temperature and can be approximated as

$$\alpha(T) = \left(10^{-5}T^2 - 3.2\times10^{-3}T + 10.439\right)\times10^{-6}, \tag{1}$$

where α denotes the coefficient of thermal expansion and T is the temperature.

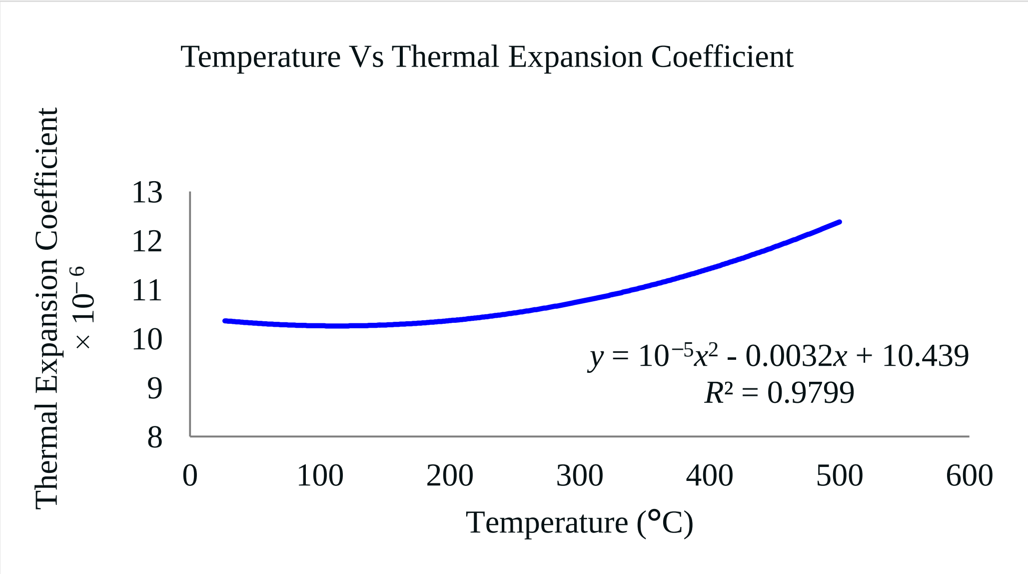

Fig. 2 Thermal Expansion coefficient of ESR Material as a function of temperature

3.2 Experimental estimation of yield strength of ESR steel

To assess the temperature dependency of yield strength of gun barrel ESR steel, tensile tests were conducted at different temperatures. The tests were conducted in universal testing machine available at Kalyani Centre for Technological Innovation (KCTI), Pune. The experimental arrangement is shown in Fig. 3.

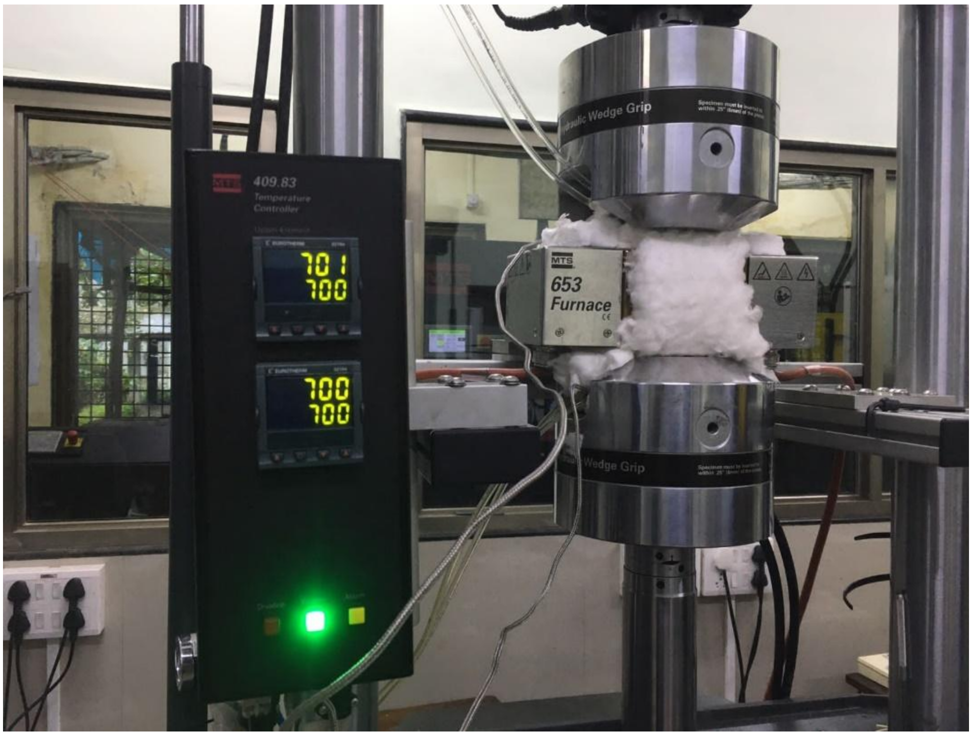

Fig 3 Universal testing machine for elevated temperature

The tensile tests were conducted considering the following:

Testing Standard used: ASTM E21-19

Specimen Dimensions as per standard: ASTM E8/E8M (schematically shown in Fig. 4)

Ratio of gauge length to diameter ≥4

Soaking time > 20 minutes

Minimum two thermocouples for gauge length < 50 mm at both ends.

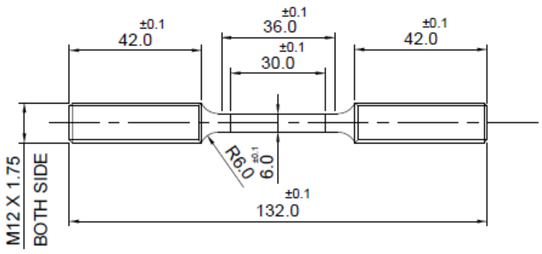

Fig. 4 Specimen Dimensions

The yield strength of ESR steel were recorded at various temperatures from the experiments and are presented in Table 3. It is to be noted that to see the repeatability, the tests were repeated for thrice for the same temperature and then the average of those three yield strengths corresponding to the same temperature are presented in Table 3.

Table 3 The yield strength (σ_Y) of the material as a function of temperature

Sr. No.	Temperature (°C)	Yield Strength (MPa)
1	27	1084.44
2	55	1075.00
3	100	1048.75
4	180	0981.50
5	200	0982.50
6	300	0930.00
7	400	0845.00
8	500	0702.50
9	550	0605.00

By fitting the experimental data points for yield strengths of ESR material from Table 3 at various temperatures in Fig. 5, it is observed that the yield strength of the material decreases with a rise in temperature. The experimental data points were fitted with a polynomial curve and approximated to second degree as

$$\sigma_Y(T) = -0.0012T^2 - 0.1854T + 1080.7, \quad (2)$$

where σ_Y denotes yield strength of the material.

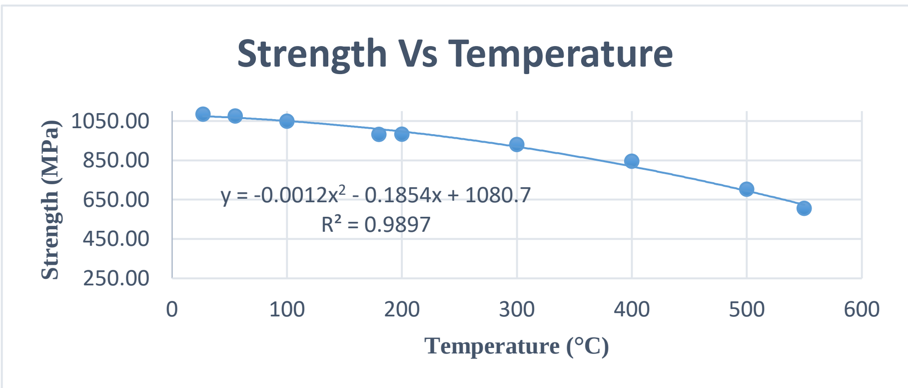

Fig. 5 Yield strength of gun barrel material (ESR steel) as a function of temperature

3.3 Experimental estimation of thermal conductivity of ESR steel

The coefficient of thermal conductivity of ESR steel was experimentally determined at different temperatures using the test facility available at High Energy Materials Research Laboratory (HEMRL), DRDO, Pune. The results are presented in Table 4. It is observed that the thermal conductivity of ESR material at different temperatures does not vary appreciably. Thus, the thermal conductivity of the gun barrel material can be considered as constant, which is the average of the value obtained for all temperatures. The estimated average value of coefficient of thermal conductivity at different temperatures is 35 W/m-K.

Table 4 The thermal conductivity (*k*) of the material as a function of temperature

Sr. No.	Temperature ($^{\circ}$C)	Thermal Conductivity, *k* (W/m-K)
1.	27	33.67
2.	28	34.01
3.	29	35.81
4.	101	34.14
5.	102	34.99
6.	103	34.76
7.	104	33.17
8.	200	36.41
9.	201	35.61
10.	202	36.09
11.	299	36.34
12.	300	35.67
13.	301	35.99
14.	399	36.01
15.	400	35.93
16.	401	34.89
17.	500	34.41
18.	501	36.74
19.	502	35.20

The Young's modulus of elasticity does not show any significant variation with temperature and its value can be taken as 208 GPa.

4. Determination of Temperature Difference Required for the Initiation of Yielding in the ESR Gun Barrel

To determine the temperature difference required for the initiation of yielding in ESR gun barrel, an elastic analysis of stresses under radial temperature difference is carried out using the temperature dependent material properties from Section 3. The required yield onset temperature difference is then obtained incorporating von Mises yield criterion.

4.1 Elastic Analysis

The stress equilibrium equation for an axisymmetric barrel is given by

$$\frac{\mathrm{d}\sigma_r}{\mathrm{d}r} + \frac{\sigma_r - \sigma_\theta}{r} = 0, \tag{3}$$

where σ_r and σ_θ denote the radial and hoop stress components, respectively. The strain-displacement relations are given by

$$\varepsilon_r = \frac{\mathrm{d}u}{\mathrm{d}r}, \qquad \varepsilon_\theta = \frac{u}{r}. \tag{4}$$

Considering the temperature dependence of the Young's modulus of elasticity (E) and coefficient of thermal expansion (α), the elastic constitutive relations can be written as

$$\varepsilon_r = \frac{1}{E(T)}\left\{\sigma_r - \nu\left(\sigma_\theta + \sigma_z\right)\right\} + \int_{T_i}^{T} \alpha(T)\,\mathrm{d}T, \tag{5}$$

$$\varepsilon_\theta = \frac{1}{E(T)}\left\{\sigma_\theta - \nu\left(\sigma_r + \sigma_z\right)\right\} + \int_{T_i}^{T} \alpha(T)\,\mathrm{d}T, \tag{6}$$

$$\varepsilon_z = \frac{1}{E(T)}\left\{\sigma_z - \nu\left(\sigma_r + \sigma_\theta\right)\right\} + \int_{T_i}^{T} \alpha(T)\,\mathrm{d}T. \tag{7}$$

Considering the ends of the cylinder are free (held by flexible supports), the axial strain can be assumed to be constant, *i.e.*, ε_z=ε_0=constant (generalized plane strain), the axial stress component can be expressed from Eq. (7) as

$$\sigma_z = \nu\left(\sigma_r + \sigma_\theta\right) + E(T)\varepsilon_0 - E(T)\int_{T_i}^{T} \alpha(T)\,\mathrm{d}T. \tag{8}$$

The strain compatibility relation provides

$$\frac{\mathrm{d}}{\mathrm{d}r}\left(r\varepsilon_\theta\right)=\varepsilon_r. \tag{9}$$

Substituting Eqs. (5) and (6) in Eq. (9) one obtains

$$\frac{\mathrm{d}}{\mathrm{d}r}\left[r\left[\frac{1}{E(T)}\left\{\sigma_\theta-\nu\left(\sigma_r+\sigma_z\right)\right\}+\int_{T_i}^{T}\alpha(T)\mathrm{d}T\right]\right]=\frac{1}{E(T)}\left\{\sigma_r-\nu\left(\sigma_\theta+\sigma_z\right)\right\}+\int_{T_i}^{T}\alpha(T)\mathrm{d}T. \tag{10}$$

Substituting the expression for σ_z from Eq. (8) in Eq. (10), one obtains

$$\begin{aligned}&\frac{\mathrm{d}}{\mathrm{d}r}\left[\frac{r}{E(T)}\left[\sigma_\theta-\nu\sigma_r-\nu\left\{\nu\left(\sigma_r+\sigma_\theta\right)+E(T)\varepsilon_0-E(T)\int_{T_i}^{T}\alpha(T)\mathrm{d}T\right\}\right]\right]+\frac{\mathrm{d}}{\mathrm{d}r}\left\{r\int_{T_i}^{T}\alpha(T)\mathrm{d}T\right\}\\&=\frac{1}{E(T)}\left\{\sigma_r-\nu\left(\sigma_\theta+\nu\left(\sigma_r+\sigma_\theta\right)+E(T)\varepsilon_0-E(T)\int_{T_i}^{T}\alpha(T)\mathrm{d}T\right)\right\}+\int_{T_i}^{T}\alpha(T)\mathrm{d}T.\end{aligned} \tag{11}$$

Use of equilibrium Eq. (3) in Eq. (11) yields

$$\begin{aligned}&\frac{\mathrm{d}}{\mathrm{d}r}\left[\frac{r}{E(T)}\left\{\sigma_r+r\frac{\mathrm{d}\sigma_r}{\mathrm{d}r}-\nu\sigma_r-\nu^2\left(\sigma_r+\sigma_r+r\frac{\mathrm{d}\sigma_r}{\mathrm{d}r}\right)-\nu E(T)\varepsilon_0+\nu E(T)\int_{T_i}^{T}\alpha(T)\mathrm{d}T\right\}\right]+\frac{\mathrm{d}}{\mathrm{d}r}\left\{r\int_{T_i}^{T}\alpha(T)\mathrm{d}T\right\}\\&=\frac{1}{E(T)}\left\{\sigma_r-\nu\left(\sigma_r+r\frac{\mathrm{d}\sigma_r}{\mathrm{d}r}\right)-\nu^2\left(\sigma_r+\sigma_r+r\frac{\mathrm{d}\sigma_r}{\mathrm{d}r}\right)-\nu E(T)\varepsilon_0+\nu E(T)\int_{T_i}^{T}\alpha(T)\mathrm{d}T\right\}+\int_{T_i}^{T}\alpha(T)\mathrm{d}T,\end{aligned}$$

$$\begin{aligned}&\frac{\mathrm{d}}{\mathrm{d}r}\left(\frac{r}{E(T)}\sigma_r\right)+\frac{\mathrm{d}}{\mathrm{d}r}\left(\frac{r^2}{E(T)}\frac{\mathrm{d}\sigma_r}{\mathrm{d}r}\right)-\nu\frac{\mathrm{d}}{\mathrm{d}r}\left(\frac{r}{E(T)}\sigma_r\right)-2\nu^2\left(\frac{r}{E(T)}\sigma_r\right)-\nu^2\frac{\mathrm{d}}{\mathrm{d}r}\left(\frac{r^2}{E(T)}\frac{\mathrm{d}\sigma_r}{\mathrm{d}r}\right)\\&-\nu\varepsilon_0\frac{\mathrm{d}}{\mathrm{d}r}(r)+\nu\frac{\mathrm{d}}{\mathrm{d}r}\left(r\int_{T_i}^{T}\alpha(T)\mathrm{d}T\right)+\frac{\mathrm{d}}{\mathrm{d}r}\left\{r\int_{T_i}^{T}\alpha(T)\mathrm{d}T\right\}\\&=\frac{\sigma_r}{E(T)}-\frac{\nu\sigma_r}{E(T)}-\frac{\nu r}{E(T)}\frac{\mathrm{d}\sigma_r}{\mathrm{d}r}-\frac{2\nu^2\sigma_r}{E(T)}-\frac{\nu^2 r}{E(T)}\frac{\mathrm{d}\sigma_r}{\mathrm{d}r}-\nu\varepsilon_0+\nu\int_{T_i}^{T}\alpha(T)\mathrm{d}T+\int_{T_i}^{T}\alpha(T)\mathrm{d}T,\end{aligned}$$

$$
\begin{aligned}
&\frac{\sigma_r}{E(T)}+r\frac{\mathrm{d}}{\mathrm{d}r}\left(\frac{\sigma_r}{E(T)}\right)+2r\frac{1}{E(T)}\frac{\mathrm{d}\sigma_r}{\mathrm{d}r}+r^2\frac{\mathrm{d}}{\mathrm{d}r}\left(\frac{1}{E(T)}\frac{\mathrm{d}\sigma_r}{\mathrm{d}r}\right)-\frac{\nu\sigma_r}{E(T)}-\nu r\frac{\mathrm{d}}{\mathrm{d}r}\left(\frac{\sigma_r}{E(T)}\right)\\
&-2\nu^2\left(\frac{\sigma_r}{E(T)}\right)-2\nu^2 r\frac{\mathrm{d}}{\mathrm{d}r}\left(\frac{\sigma_r}{E(T)}\right)-\frac{2r\nu^2}{E(T)}\frac{\mathrm{d}\sigma_r}{\mathrm{d}r}-r^2\nu^2\frac{\mathrm{d}}{\mathrm{d}r}\left(\frac{1}{E(T)}\frac{\mathrm{d}\sigma_r}{\mathrm{d}r}\right)-\nu\varepsilon_0+\nu\int_{T_i}^{T}\alpha(T)\mathrm{d}T\\
&+r\nu\frac{\mathrm{d}}{\mathrm{d}r}\left(\int_{T_i}^{T}\alpha(T)\mathrm{d}T\right)+\int_{T_i}^{T}\alpha(T)\mathrm{d}T+r\frac{\mathrm{d}}{\mathrm{d}r}\left\{\int_{T_i}^{T}\alpha(T)\mathrm{d}T\right\}\\
&=\frac{\sigma_r}{E(T)}-\frac{\nu\sigma_r}{E(T)}-\frac{\nu r}{E(T)}\frac{\mathrm{d}\sigma_r}{\mathrm{d}r}-\frac{2\nu^2\sigma_r}{E(T)}-\frac{\nu^2 r}{E(T)}\frac{\mathrm{d}\sigma_r}{\mathrm{d}r}-\nu\varepsilon_0+\nu\int_{T_i}^{T}\alpha(T)\mathrm{d}T+\int_{T_i}^{T}\alpha(T)\mathrm{d}T,
\end{aligned}
$$

$$
\begin{aligned}
&r\frac{\mathrm{d}}{\mathrm{d}r}\left(\frac{\sigma_r}{E(T)}\right)+2r\frac{1}{E(T)}\frac{\mathrm{d}\sigma_r}{\mathrm{d}r}+r^2\frac{\mathrm{d}}{\mathrm{d}r}\left(\frac{1}{E(T)}\frac{\mathrm{d}\sigma_r}{\mathrm{d}r}\right)-\nu r\frac{\mathrm{d}}{\mathrm{d}r}\left(\frac{\sigma_r}{E(T)}\right)\\
&-2\nu^2 r\frac{\mathrm{d}}{\mathrm{d}r}\left(\frac{\sigma_r}{E(T)}\right)-\frac{2r\nu^2}{E(T)}\frac{\mathrm{d}\sigma_r}{\mathrm{d}r}-r^2\nu^2\frac{\mathrm{d}}{\mathrm{d}r}\left(\frac{1}{E(T)}\frac{\mathrm{d}\sigma_r}{\mathrm{d}r}\right)+r\nu\frac{\mathrm{d}}{\mathrm{d}r}\left(\int_{T_i}^{T}\alpha(T)\mathrm{d}T\right)\\
&+r\frac{\mathrm{d}}{\mathrm{d}r}\left\{\int_{T_i}^{T}\alpha(T)\mathrm{d}T\right\}=-\frac{\nu r}{E(T)}\frac{\mathrm{d}\sigma_r}{\mathrm{d}r}-\frac{\nu^2 r}{E(T)}\frac{\mathrm{d}\sigma_r}{\mathrm{d}r},
\end{aligned}
$$

$$
\begin{aligned}
&\frac{r^2}{E(T)}\left(1-\nu^2\right)\frac{\mathrm{d}^2\sigma_r}{\mathrm{d}r^2}+\frac{3r}{E(T)}\frac{\mathrm{d}\sigma_r}{\mathrm{d}r}-\nu^2\frac{3r}{E(T)}\frac{\mathrm{d}\sigma_r}{\mathrm{d}r}+r\sigma_r\left(1-\nu-2\nu^2\right)\frac{\mathrm{d}}{\mathrm{d}r}\left(\frac{1}{E(T)}\right)\\
&+r^2\frac{\mathrm{d}\sigma_r}{\mathrm{d}r}\left(1-\nu^2\right)\frac{\mathrm{d}}{\mathrm{d}r}\left(\frac{1}{E(T)}\right)=-(1+\nu)r\frac{\mathrm{d}}{\mathrm{d}r}\left\{\int_{T_i}^{T}\alpha(T)\mathrm{d}T\right\},
\end{aligned}
$$

$$
\begin{aligned}
&\frac{r^2}{E(T)}(1+\nu)(1-\nu)\frac{\mathrm{d}^2\sigma_r}{\mathrm{d}r^2}+\frac{3r}{E(T)}(1+\nu)(1-\nu)\frac{\mathrm{d}\sigma_r}{\mathrm{d}r}+(1+\nu)(1-2\nu)r\sigma_r\left[-\frac{\frac{\mathrm{d}E(T)}{\mathrm{d}r}}{\left\{E(T)\right\}^2}\right]\\
&+(1+\nu)(1-\nu)r^2\frac{\mathrm{d}\sigma_r}{\mathrm{d}r}\left[-\frac{\frac{\mathrm{d}E(T)}{\mathrm{d}r}}{\left\{E(T)\right\}^2}\right]=-(1+\nu)r\frac{\mathrm{d}}{\mathrm{d}r}\left\{\int_{T_i}^{T}\alpha(T)\mathrm{d}T\right\},
\end{aligned}
$$

$$\frac{r^2}{E(T)}(1-\nu)\frac{\mathrm{d}^2\sigma_r}{\mathrm{d}r^2}+\frac{3r}{E(T)}(1-\nu)\frac{\mathrm{d}\sigma_r}{\mathrm{d}r}-(1-2\nu)r\sigma_r\left[\frac{\frac{\mathrm{d}E(T)}{\mathrm{d}r}}{\{E(T)\}^2}\right]$$

$$-(1-\nu)r^2\frac{\mathrm{d}\sigma_r}{\mathrm{d}r}\left[\frac{\frac{\mathrm{d}E(T)}{\mathrm{d}r}}{\{E(T)\}^2}\right]=-r\frac{\mathrm{d}}{\mathrm{d}r}\left\{\int_{T_i}^{T}\alpha(T)\mathrm{d}T\right\},$$

$$\frac{\mathrm{d}^2\sigma_r}{\mathrm{d}r^2}+\frac{3}{r}\frac{\mathrm{d}\sigma_r}{\mathrm{d}r}-\left(\frac{1-2\nu}{1-\nu}\right)\frac{\sigma_r}{r}\left\{\frac{\frac{\mathrm{d}E(T)}{\mathrm{d}r}}{E(T)}\right\}-\frac{\mathrm{d}\sigma_r}{\mathrm{d}r}\left\{\frac{\frac{\mathrm{d}E(T)}{\mathrm{d}r}}{E(T)}\right\}=-\frac{E(T)}{(1-\nu)r}\frac{\mathrm{d}}{\mathrm{d}r}\left\{\int_{T_i}^{T}\alpha(T)\mathrm{d}T\right\},$$

$$\frac{\mathrm{d}^2\sigma_r}{\mathrm{d}r^2}+\left(\frac{3}{r}-\frac{E'(T)}{E(T)}\right)\frac{\mathrm{d}\sigma_r}{\mathrm{d}r}-\left(\frac{1-2\nu}{1-\nu}\right)\frac{\sigma_r}{r}\frac{E'(T)}{E(T)}=-\frac{E(T)}{(1-\nu)r}\frac{\mathrm{d}}{\mathrm{d}r}\left\{\int_{T_i}^{T}\alpha(T)\mathrm{d}T\right\}, \tag{12}$$

where

$$E'(T)=\frac{\mathrm{d}E(T)}{\mathrm{d}r}.$$

One can obtain the radial stress distribution in an axisymmetric elastic cylinder by solving Eq. (12) with suitable boundary conditions for temperature dependent material properties. The solution for hoop stress is then obtained using Eq. (3) as

$$\sigma_\theta=\frac{\mathrm{d}}{\mathrm{d}r}(r\sigma_r) \tag{13}$$

The axial stress distribution can be obtained from Eq. (8).

4.2 Temperature Distribution

It is assumed that the heating of the outer wall of the cylinder takes place gradually reaching to a certain predefined temperature, while keeping the inner surface at a constant temperature. The steady state heat conduction equation can be expressed as

$$\frac{1}{r}\frac{\mathrm{d}}{\mathrm{d}r}\left\{rk(T)\frac{\mathrm{d}T}{\mathrm{d}r}\right\}=0. \tag{14}$$

It is experimentally verified that the thermal conductivity k for gun barrel steel remains almost constant upon increasing temperature. Thus, here it is considered k as constant. Thus, solving Eq. (14), the temperature distribution is obtained as

$$T(r) = T_a + (T_b - T_a)\frac{\ln\left(\frac{r}{a}\right)}{\ln\left(\frac{b}{a}\right)}, \tag{15}$$

where T_a is the temperature at the inner surface, T_b is the temperature at the outer surface of the cylinder.

4.3 Elastic stress solutions for ESR cylinder

The coefficient of thermal expansion of the gun barrel material, ESR steel is taken to be as a quadratic function of temperature as given in Eq. (1) and expressed in the following generic form

$$\alpha(T) = A_1 T^2 + A_2 T + A_3, \tag{16}$$

where the coefficients A_1, A_2 and A_3 can be easily comprehend from Eq. (1). In Eq. (16), T is given by Eq. (15) and α is measured in /°C.

As mentioned in Section 3, the Young's modulus of elasticity, E does not vary much with temperature, in Eq. (12), the temperature dependency of Young's modulus of elasticity can be neglected. Thus, Eq. (12) reduces to

$$\frac{\mathrm{d}^2\sigma_r}{\mathrm{d}r^2} + \frac{3}{r}\frac{\mathrm{d}\sigma_r}{\mathrm{d}r} = -\frac{E}{(1-\nu)r}\frac{\mathrm{d}}{\mathrm{d}r}\left\{\int_{T_i}^{T}\alpha(T)\,\mathrm{d}T\right\}. \tag{17}$$

Substituting $\alpha(T)$ and then T in Eq. (17) and solving the resulting equation, the solution of radial stress is obtained as

$$\sigma_r = C_1 + \frac{C_2}{r^2} + \frac{E(T_b - T_a)}{2(1-\nu)\ln\left(\frac{b}{a}\right)}\left\{\frac{A_1 T_a^{\,2}}{2} + \frac{A_2}{2}T_a + \frac{A_3}{2} - T_a \ln r\left(A_1 T_a + A_2\right) - A_3 \ln r\right\}$$

$$+\frac{E(T_b - T_a)^2}{2(1-\nu)\left\{\ln\left(\frac{b}{a}\right)\right\}^2}\left[\left\{\ln\left(\frac{r}{a}\right) - \frac{1}{2}\right\}\left(A_1 T_a + \frac{A_2}{2}\right) - A_1 T_a \ln r\left\{2\ln\left(\frac{r}{a}\right) - \ln r\right\} - A_2\left\{\ln\left(\frac{r}{a}\right)\ln r - \frac{(\ln r)^2}{2}\right\}\right] \tag{18}$$

$$+\frac{E(T_b - T_a)^3}{2(1-\nu)\left\{\ln\left(\frac{b}{a}\right)\right\}^3}A_1\left[\left\{\ln\left(\frac{r}{a}\right)\right\}^2\left(\frac{1}{2} - \ln r\right) + \ln\left(\frac{r}{a}\right)\left\{(\ln r)^2 - \frac{1}{2}\right\} - \frac{(\ln r)^3}{3} + \frac{1}{4}\right].$$

where C_1 and C_2 are integration constant and can be evaluated using the following boundary conditions (BC):

(i) at $r=a$, $\sigma_r=0$,

(ii) at $r=b$, $\sigma_r=0$.

Use of B.C. (i) in Eq. (18) provides

$$C_1 + \frac{C_2}{a^2} + \frac{E(T_b - T_a)}{2(1-\nu)\ln\left(\frac{b}{a}\right)}\left\{\frac{A_1 T_a^{\,2}}{2} + \frac{A_2}{2}T_a + \frac{A_3}{2} - T_a \ln a\left(A_1 T_a + A_2\right) - A_3 \ln a\right\}$$

$$+\frac{E(T_b - T_a)^2}{2(1-\nu)\left\{\ln\left(\frac{b}{a}\right)\right\}^2}\left\{-\frac{1}{2}\left(A_1 T_a + \frac{A_2}{2}\right) + A_1 T_a (\ln a)^2 + A_2\frac{(\ln a)^2}{2}\right\}$$

$$+\frac{E(T_b - T_a)^3}{2(1-\nu)\left\{\ln\left(\frac{b}{a}\right)\right\}^3}A_1\left\{-\frac{(\ln a)^3}{3} + \frac{1}{4}\right\} = 0,$$

$$C_2 = -C_1 a^2 - \frac{E(T_b - T_a)a^2}{2(1-\nu)\ln\left(\frac{b}{a}\right)}\left\{\frac{A_1 T_a^{\,2}}{2} + \frac{A_2}{2}T_a + \frac{A_3}{2} - T_a \ln a\left(A_1 T_a + A_2\right) - A_3 \ln a\right\}$$

$$-\frac{E(T_b - T_a)^2 a^2}{2(1-\nu)\left\{\ln\left(\frac{b}{a}\right)\right\}^2}\left\{-\frac{1}{2}\left(A_1 T_a + \frac{A_2}{2}\right) + A_1 T_a (\ln a)^2 + A_2\frac{(\ln a)^2}{2}\right\} \tag{19}$$

$$-\frac{E(T_b - T_a)^3 a^2}{2(1-\nu)\left\{\ln\left(\frac{b}{a}\right)\right\}^3}A_1\left\{-\frac{(\ln a)^3}{3} + \frac{1}{4}\right\}.$$

Use of B.C. (ii) in Eq. (18) provides

$$C_1+\frac{C_2}{b^2}+\frac{E\left(T_b-T_a\right)}{2(1-\nu)\ln\left(\frac{b}{a}\right)}\left\{\frac{A_1T_a^{\,2}}{2}+\frac{A_2}{2}T_a+\frac{A_3}{2}-T_a\ln b\left(A_1T_a+A_2\right)-A_3\ln b\right\}$$
$$+\frac{E\left(T_b-T_a\right)^2}{2(1-\nu)\left\{\ln\left(\frac{b}{a}\right)\right\}^2}\left[\left\{\ln\left(\frac{b}{a}\right)-\frac{1}{2}\right\}\left(A_1T_a+\frac{A_2}{2}\right)-A_1T_a\ln b\left\{2\ln\left(\frac{b}{a}\right)-\ln b\right\}-A_2\left\{\ln\left(\frac{b}{a}\right)\ln b-\frac{(\ln b)^2}{2}\right\}\right] \qquad (20)$$
$$+\frac{E\left(T_b-T_a\right)^3}{2(1-\nu)\left\{\ln\left(\frac{b}{a}\right)\right\}^3}A_1\left[\left\{\ln\left(\frac{b}{a}\right)\right\}^2\left(\frac{1}{2}-\ln b\right)+\ln\left(\frac{b}{a}\right)\left\{(\ln b)^2-\frac{1}{2}\right\}-\frac{(\ln b)^3}{3}+\frac{1}{4}\right]=0.$$

Substituting the value of C_2 from Eq. (19) in Eq. (20), one obtains

$$C_1\left(1-\frac{a^2}{b^2}\right)=\frac{E\left(T_b-T_a\right)a^2}{2(1-\nu)\ln\left(\frac{b}{a}\right)b^2}\left\{\frac{A_1T_a^{\,2}}{2}+\frac{A_2}{2}T_a+\frac{A_3}{2}-T_a\ln a\left(A_1T_a+A_2\right)-A_3\ln a\right\}$$
$$+\frac{E\left(T_b-T_a\right)^2a^2}{2(1-\nu)\left\{\ln\left(\frac{b}{a}\right)\right\}^2b^2}\left\{-\frac{1}{2}\left(A_1T_a+\frac{A_2}{2}\right)+A_1T_a(\ln a)^2+A_2\frac{(\ln a)^2}{2}\right\}+\frac{E\left(T_b-T_a\right)^3a^2}{2(1-\nu)\left\{\ln\left(\frac{b}{a}\right)\right\}^3b^2}A_1\left\{-\frac{(\ln a)^3}{3}+\frac{1}{4}\right\}$$
$$-\frac{E\left(T_b-T_a\right)}{2(1-\nu)\ln\left(\frac{b}{a}\right)}\left\{\frac{A_1T_a^{\,2}}{2}+\frac{A_2}{2}T_a+\frac{A_3}{2}-T_a\ln b\left(A_1T_a+A_2\right)-A_3\ln b\right\}$$
$$-\frac{E\left(T_b-T_a\right)^2}{2(1-\nu)\left\{\ln\left(\frac{b}{a}\right)\right\}^2}\left[\left\{\ln\left(\frac{b}{a}\right)-\frac{1}{2}\right\}\left(A_1T_a+\frac{A_2}{2}\right)-A_1T_a\ln b\left\{2\ln\left(\frac{b}{a}\right)-\ln b\right\}-A_2\left\{\ln\left(\frac{b}{a}\right)\ln b-\frac{(\ln b)^2}{2}\right\}\right]$$
$$-\frac{E\left(T_b-T_a\right)^3}{2(1-\nu)\left\{\ln\left(\frac{b}{a}\right)\right\}^3}A_1\left[\left\{\ln\left(\frac{b}{a}\right)\right\}^2\left(\frac{1}{2}-\ln b\right)+\ln\left(\frac{b}{a}\right)\left\{(\ln b)^2-\frac{1}{2}\right\}-\frac{(\ln b)^3}{3}+\frac{1}{4}\right],$$

$$C_1\left(1-\frac{a^2}{b^2}\right)=\frac{E\left(T_b-T_a\right)}{2(1-\nu)\ln\left(\frac{b}{a}\right)}\left\{\left(\frac{a^2}{b^2}-1\right)\left(\frac{A_1T_a^{\,2}}{2}+\frac{A_2}{2}T_a+\frac{A_3}{2}\right)-T_a\left(A_1T_a+A_2\right)\left(\frac{a^2}{b^2}\ln a-\ln b\right)-A_3\frac{a^2}{b^2}\ln a+A_3\ln b\right\}$$
$$+\frac{E\left(T_b-T_a\right)^2}{2(1-\nu)\left\{\ln\left(\frac{b}{a}\right)\right\}^2}\left[\begin{aligned}&\left(A_1T_a+\frac{A_2}{2}\right)\left\{\frac{1}{2}\left(1-\frac{a^2}{b^2}\right)-\ln\left(\frac{b}{a}\right)\right\}+A_1T_a\left\{\frac{a^2}{b^2}(\ln a)^2-(\ln b)^2+2\ln b\ln\left(\frac{b}{a}\right)\right\}\\&+A_2\frac{(\ln a)^2}{2}\frac{a^2}{b^2}+A_2\left\{\ln\left(\frac{b}{a}\right)\ln b-\frac{(\ln b)^2}{2}\right\}\end{aligned}\right]$$
$$+\frac{E\left(T_b-T_a\right)^3}{2(1-\nu)\left\{\ln\left(\frac{b}{a}\right)\right\}^3}A_1\left[-\frac{a^2}{b^2}\frac{(\ln a)^3}{3}+\frac{1}{4}\left(\frac{a^2}{b^2}-1\right)-\left\{\ln\left(\frac{b}{a}\right)\right\}^2\left(\frac{1}{2}-\ln b\right)-\ln\left(\frac{b}{a}\right)\left\{(\ln b)^2-\frac{1}{2}\right\}+\frac{(\ln b)^3}{3}\right],$$

$$C_1 = \frac{P}{\left(1-\frac{a^2}{b^2}\right)}, \tag{21}$$

where

$$\begin{aligned}
P &= \frac{E(T_b-T_a)}{2(1-\nu)\ln\left(\frac{b}{a}\right)}\left\{\left(\frac{a^2}{b^2}-1\right)\left(\frac{A_1T_a^{\,2}}{2}+\frac{A_2}{2}T_a+\frac{A_3}{2}\right)-T_a\left(A_1T_a+A_2\right)\left(\frac{a^2}{b^2}\ln a-\ln b\right)-A_3\frac{a^2}{b^2}\ln a+A_3\ln b\right\}\\
&+\frac{E(T_b-T_a)^2}{2(1-\nu)\left\{\ln\left(\frac{b}{a}\right)\right\}^2}\left[\begin{array}{l}\left(A_1T_a+\frac{A_2}{2}\right)\left\{\frac{1}{2}\left(1-\frac{a^2}{b^2}\right)-\ln\left(\frac{b}{a}\right)\right\}+A_1T_a\left\{\frac{a^2}{b^2}(\ln a)^2-(\ln b)^2+2\ln b\ln\left(\frac{b}{a}\right)\right\}\\ +A_2\frac{(\ln a)^2}{2}\frac{a^2}{b^2}+A_2\left\{\ln\left(\frac{b}{a}\right)\ln b-\frac{(\ln b)^2}{2}\right\}\end{array}\right]\\
&+\frac{E(T_b-T_a)^3}{2(1-\nu)\left\{\ln\left(\frac{b}{a}\right)\right\}^3}A_1\left[-\frac{a^2}{b^2}\frac{(\ln a)^3}{3}+\frac{1}{4}\left(\frac{a^2}{b^2}-1\right)-\left\{\ln\left(\frac{b}{a}\right)\right\}^2\left(\frac{1}{2}-\ln b\right)-\ln\left(\frac{b}{a}\right)\left\{(\ln b)^2-\frac{1}{2}\right\}+\frac{(\ln b)^3}{3}\right].
\end{aligned} \tag{22}$$

Knowing C_1 from Eq. (21), C_2 can be obtained from Eq. (19).

The solution for hoop stress is obtained by using the equilibrium equation as

$$\begin{aligned}
\sigma_\theta &= C_1+\frac{C_2}{r^2}+\frac{E(T_b-T_a)}{2(1-\nu)\ln\left(\frac{b}{a}\right)}\left\{\frac{A_1T_a^{\,2}}{2}+\frac{A_2}{2}T_a+\frac{A_3}{2}-T_a\ln r\left(A_1T_a+A_2\right)-A_3\ln r\right\}\\
&+\frac{E(T_b-T_a)^2}{2(1-\nu)\left\{\ln\left(\frac{b}{a}\right)\right\}^2}\left[\left\{\ln\left(\frac{r}{a}\right)-\frac{1}{2}\right\}\left(A_1T_a+\frac{A_2}{2}\right)-A_1T_a\ln r\left\{2\ln\left(\frac{r}{a}\right)-\ln r\right\}-A_2\left\{\ln\left(\frac{r}{a}\right)\ln r-\frac{(\ln r)^2}{2}\right\}\right]\\
&+\frac{E(T_b-T_a)^3}{2(1-\nu)\left\{\ln\left(\frac{b}{a}\right)\right\}^3}A_1\left[\left\{\ln\left(\frac{r}{a}\right)\right\}^2\left(\frac{1}{2}-\ln r\right)+\ln\left(\frac{r}{a}\right)\left\{(\ln r)^2-\frac{1}{2}\right\}-\frac{(\ln r)^3}{3}+\frac{1}{4}\right]\\
&-\frac{2C_2}{r^2}-\frac{E(T_b-T_a)}{2(1-\nu)\ln\left(\frac{b}{a}\right)}\left\{T_a\left(A_1T_a+A_2\right)+A_3\right\}+\frac{E(T_b-T_a)^2}{2(1-\nu)\left\{\ln\left(\frac{b}{a}\right)\right\}^2}\left[\begin{array}{l}\left(A_1T_a+\frac{A_2}{2}\right)-A_1T_a\left\{2\ln\left(\frac{r}{a}\right)-\ln r\right\}\\ -A_1T_a\ln r-A_2\ln\left(\frac{r}{a}\right)\end{array}\right]\\
&+\frac{E(T_b-T_a)^3}{2(1-\nu)\left\{\ln\left(\frac{b}{a}\right)\right\}^3}A_1\left[2\ln\left(\frac{r}{a}\right)\left(\frac{1}{2}-\ln r\right)-\left\{\ln\left(\frac{r}{a}\right)\right\}^2+2\ln r\ln\left(\frac{r}{a}\right)+\left\{(\ln r)^2-\frac{1}{2}\right\}-(\ln r)^2\right].
\end{aligned}$$

$$\sigma_\theta = C_1 - \frac{C_2}{r^2} + \frac{E(T_b - T_a)}{2(1-\nu)\ln\left(\frac{b}{a}\right)}\left\{\frac{A_1T_a^2}{2} + \frac{A_2}{2}T_a + \frac{A_3}{2} - T_a(A_1T_a + A_2)(1+\ln r) - A_3(1+\ln r)\right\}$$

$$+\frac{E(T_b - T_a)^2}{2(1-\nu)\left\{\ln\left(\frac{b}{a}\right)\right\}^2}\begin{bmatrix}\left(A_1T_a + \frac{A_2}{2}\right)\left\{1+\ln\left(\frac{r}{a}\right) - \frac{1}{2}\right\} - 2A_1T_a\ln\left(\frac{r}{a}\right)(1+\ln r) \\ +A_1T_a(\ln r)^2 - A_2\ln\left(\frac{r}{a}\right)(1+\ln r) + A_2\frac{(\ln r)^2}{2}\end{bmatrix} \tag{23}$$

$$+\frac{E(T_b - T_a)^3}{2(1-\nu)\left\{\ln\left(\frac{b}{a}\right)\right\}^3}A_1\left[-\left\{\ln\left(\frac{r}{a}\right)\right\}^2\left(\frac{1}{2}+\ln r\right) + 2\ln\left(\frac{r}{a}\right)\left(\frac{1}{2}-\ln r\right) + \ln\left(\frac{r}{a}\right)\left\{(\ln r)^2 - \frac{1}{2} + 2\ln r\right\} - \frac{(\ln r)^3}{3} - \frac{1}{4}\right].$$

The axial stress distribution can be obtained by substituting the values of σ_r and σ_θ from Eqs. (16) and (21) in Eq. (6) as

$$\sigma_z = \nu(\sigma_r + \sigma_\theta) + E(T)\varepsilon_0 - E(T)\int_{T_i}^{T}\alpha(T)\,\mathrm{d}T,$$

$$\sigma_z = 2\nu C_1 + \frac{E\nu(T_b - T_a)}{2(1-\nu)\ln\left(\frac{b}{a}\right)}\left\{A_1T_a^2 + A_2T_a + A_3 - 2T_a\ln r(A_1T_a + A_2) - 2A_3\ln r - T_a(A_1T_a + A_2) - A_3\right\}$$

$$+\frac{E\nu(T_b - T_a)^2}{2(1-\nu)\left\{\ln\left(\frac{b}{a}\right)\right\}^2}\left[2\ln\left(\frac{r}{a}\right)\left(A_1T_a + \frac{A_2}{2}\right) + 2A_1T_a(\ln r)^3 - 2A_1T_a\ln\left(\frac{r}{a}\right) - A_2\left\{\ln\left(\frac{r}{a}\right)(1+2\ln r)\right\}\right]$$

$$+\frac{E\nu(T_b - T_a)^3}{2(1-\nu)\left\{\ln\left(\frac{b}{a}\right)\right\}^3}A_1\left[-2\ln r\left\{\ln\left(\frac{r}{a}\right)\right\}^2 + 2(\ln r)^2\ln\left(\frac{r}{a}\right) - 2\frac{(\ln r)^3}{3}\right] + E\varepsilon_0$$

$$-E\left\{\frac{A_1}{3}\left(T^3 - T_i^3\right) + \frac{A_2}{2}\left(T^2 - T_i^2\right) + A_3(T - T_i)\right\},$$

$$\sigma_z = 2\nu C_1 + \frac{E\nu\left(T_b - T_a\right)}{2(1-\nu)\ln\left(\frac{b}{a}\right)}\left\{A_1 T_a^{\,2} + A_2 T_a + A_3 - 2T_a \ln r\left(A_1 T_a + A_2\right) - 2A_3 \ln r - T_a\left(A_1 T_a + A_2\right) - A_3\right\}$$

$$+\frac{E\nu\left(T_b - T_a\right)^2}{2(1-\nu)\left\{\ln\left(\frac{b}{a}\right)\right\}^2}\left[2\ln\left(\frac{r}{a}\right)\left(A_1 T_a + \frac{A_2}{2}\right) + 2A_1 T_a\left(\ln r\right)^3 - 2A_1 T_a \ln\left(\frac{r}{a}\right) - A_2\left\{\ln\left(\frac{r}{a}\right)(1 + 2\ln r)\right\}\right]$$

$$+\frac{E\nu\left(T_b - T_a\right)^3}{2(1-\nu)\left\{\ln\left(\frac{b}{a}\right)\right\}^3}A_1\left[-2\ln r\left\{\ln\left(\frac{r}{a}\right)\right\}^2 + 2\left(\ln r\right)^2 \ln\left(\frac{r}{a}\right) - 2\frac{\left(\ln r\right)^3}{3}\right] + E\varepsilon_0 \quad (24)$$

$$-E\left[\frac{A_1}{3}\left\{\left(T_a + \left(T_b - T_a\right)\frac{\ln\left(\frac{r}{a}\right)}{\ln\left(\frac{b}{a}\right)}\right)^3 - T_i^3\right\} + \frac{A_2}{2}\left\{\left(T_a + \left(T_b - T_a\right)\frac{\ln\left(\frac{r}{a}\right)}{\ln\left(\frac{b}{a}\right)}\right)^2 - T_i^2\right\} + A_3\left(T_a + \left(T_b - T_a\right)\frac{\ln\left(\frac{r}{a}\right)}{\ln\left(\frac{b}{a}\right)} - T_i\right)\right].$$

$$\sigma_z = 2\nu C_1 + \frac{E\nu\left(T_b - T_a\right)}{2(1-\nu)\ln\left(\frac{b}{a}\right)}\left\{A_1 T_a^{\,2} + A_2 T_a + A_3 - 2T_a \ln r\left(A_1 T_a + A_2\right) - 2A_3 \ln r - T_a\left(A_1 T_a + A_2\right) - A_3\right\}$$

$$+\frac{E\nu\left(T_b - T_a\right)^2}{2(1-\nu)\left\{\ln\left(\frac{b}{a}\right)\right\}^2}\left[2A_1 T_a\left(\ln r\right)^3 - 2A_2 \ln\left(\frac{r}{a}\right)\ln r\right] \quad (25)$$

$$+\frac{E\nu\left(T_b - T_a\right)^3}{2(1-\nu)\left\{\ln\left(\frac{b}{a}\right)\right\}^3}A_1\left[-2\ln r\left\{\ln\left(\frac{r}{a}\right)\right\}^2 + 2\left(\ln r\right)^2 \ln\left(\frac{r}{a}\right) - 2\frac{\left(\ln r\right)^3}{3}\right] + E\varepsilon_0$$

$$-E\left[\frac{A_1}{3}\left\{\left(T_a + \left(T_b - T_a\right)\frac{\ln\left(\frac{r}{a}\right)}{\ln\left(\frac{b}{a}\right)}\right)^3 - T_i^3\right\} + \frac{A_2}{2}\left\{\left(T_a + \left(T_b - T_a\right)\frac{\ln\left(\frac{r}{a}\right)}{\ln\left(\frac{b}{a}\right)}\right)^2 - T_i^2\right\} + A_3\left(T_a + \left(T_b - T_a\right)\frac{\ln\left(\frac{r}{a}\right)}{\ln\left(\frac{b}{a}\right)} - T_i\right)\right].$$

To obtain the constant axial strain, the following free end condition is used:

$$\int_a^b \sigma_z\left(2\pi r\right)\mathrm{d}r = 0, \quad \int_a^b r\sigma_z \mathrm{d}r = 0. \quad (26)$$

Substituting Eq. (22) in Eq. (23) one can evaluate the constant axial strain ε_0.

4.4 The yield onset temperature difference required for the initiation of yielding

For the initiation of yielding, von Mises yield criteria is assumed. As yielding initiates at the inner radius *a*, one can write the condition for yield onset following von Mises criteria as

$$\left\{\left(\sigma_r-\sigma_\theta\right)^2+\left(\sigma_\theta-\sigma_z\right)^2+\left(\sigma_z-\sigma_r\right)^2\right\}\Big|_{r=a}=2\left\{\sigma_Y\left(T\right)\right\}^2, \tag{27}$$

where $\sigma_Y(T)$ is given by Eq. (2) for ESR steel. Here, it is considered that the ESR barrel has an inner radius a=40 mm and outer radius b=120 mm. Now, substituting the solutions for σ_r, σ_θ and σ_z in Eq. (27) and evaluating it at $r=a$=40 mm, the solution for yield onset temperature difference for the present ESR barrel is obtained as $(T_b–T_a)_Y$= 505 ºC. Thus, for achieving thermal autofrettage in the barrel, one needs to maintain a radial temperature difference which is greater than 505 ºC.

5. Layout Design of Thermal Autofrettage Setup for Gun Barrels

It is to be mentioned that initially the temperature dependent properties of ESR steel were not known. Initially it was assumed that the properties of ESR steel are not varying drastically with temperature. However, after actual experimentation it has been noticed that the thermomechanical properties of ESR steel from the perspective of thermal autofrettage is strongly dependent on temperature. Based on the properties available for the material at room temperature and assuming the coefficient of thermal expansion of ESR steel to be of the same order as that of the other steel grades, e.g., SS304, *i.e.*, 17.2×10^{-6}/ºC, the yield onset temperature difference for an ESR barrel with wall thickness ratio b/a=3 was evaluated as 198 ºC. The actual experimentation shows that the ESR steel used to manufacture large calibre gun barrel has properties that are drastically different than what was assumed and using the actual temperature dependent material behaviour, it is found that the actual yield onset temperature difference is 505 ºC (refer Section 4.4). A comparison of the initially considered material properties of ESR steel and actual temperature dependent properties are presented in Table 5.

Based on the initial consideration of temperature independent material properties of ESR steel, an experimental setup was conceived to be developed in-house as shown in Fig. 6. As the temperature difference required to achieve thermal autofrettage based on the initial consideration was not very large, it was thought to be created using the set up shown in Fig. 6. In the proposed set up shown in Fig. 6, the barrel to be autofrettaged was considered to be held vertical to avoid sagging as the barrel tube is sufficiently long of the order of 0.5 to 1 m. The set up consists of three basic units, *viz*., the heating system, the cooling system and the control unit.

Table 5 Comparison of different parameters of thermal autofrettage for ESR barrel between initially considered properties and after actual experimentation

Parameters	**Initial consideration for proposal**	**After actual determination of temperature dependent properties**
Yield strength (σ_Y)	950 MPa	$\sigma_Y(T)=0.001T^2 - 0.2921T + 1089.7$
Thermal coefficient of expansion (α)	17.2×10^{-6}/°C	$\alpha(T) = 10^{-6}(10^{-5}T^2 - 3.2\times10^{-3}T + 10.439)$
Thermal conductivity (k)	35 W/mK	35 W/mK
Estimated temperature difference (ΔT) for initiation of yielding	198 °C	505°C
Power requirement (kW)	20	100

The actual determination of temperature dependent thermomechanical properties leads to the requirement of a very high radial temperature difference which is more than 505 ºC. This poses a difficulty to achieve thermal autofrettage with the initially conceived design of the experimental set up. In order to maintain such a high temperature difference the experimental set up needs to be incorporated with a pit furnace of 100 kW capacity for a barrel with a=40 mm and b=120 mm and length L=750 mm. Further, the tempering temperature of the ESR material is of the order of 580 ºC. This again put an additional constraint that the temperature of the outer wall of the barrel should not be allowed to reach beyond 580 ºC. Thus, to maintain a desired temperature difference for thermal autofrettage without reaching to tempering temperature of the material at the outer wall of the barrel, it is proposed to incorporate a chiller unit. The chiller unit will help in circulating the cold fluid (mixture of water and ethylene glycol) at sufficiently low temperature that will keep the inner wall of the barrel at a very low temperature. Thus, the desired high temperature difference required for the thermal autofrettage of ESR barrel can be achieved easily. Based on this new requirements, the experimental set up is modified and the CAD design layout of the setup is shown in Fig. 7.

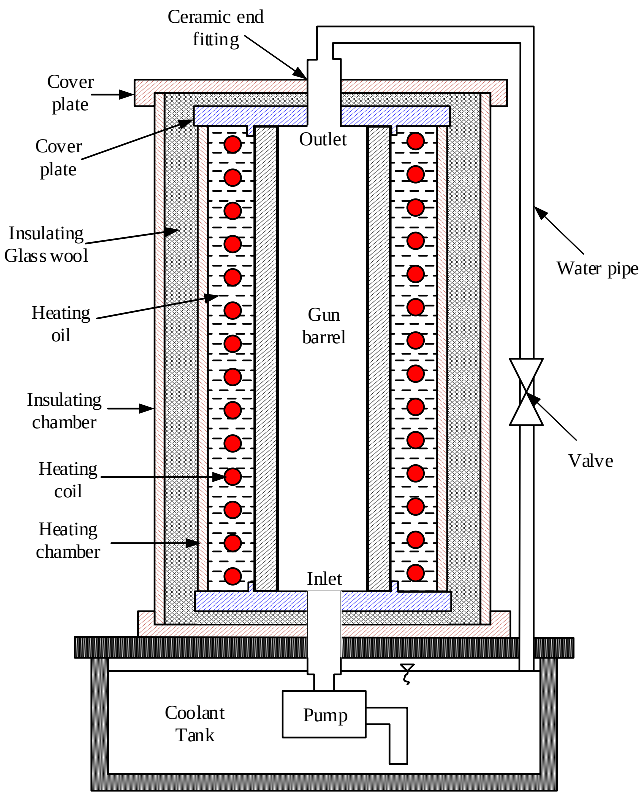

Fig. 6 Initial concept of the experimental set up for thermal autofrettage of barrel

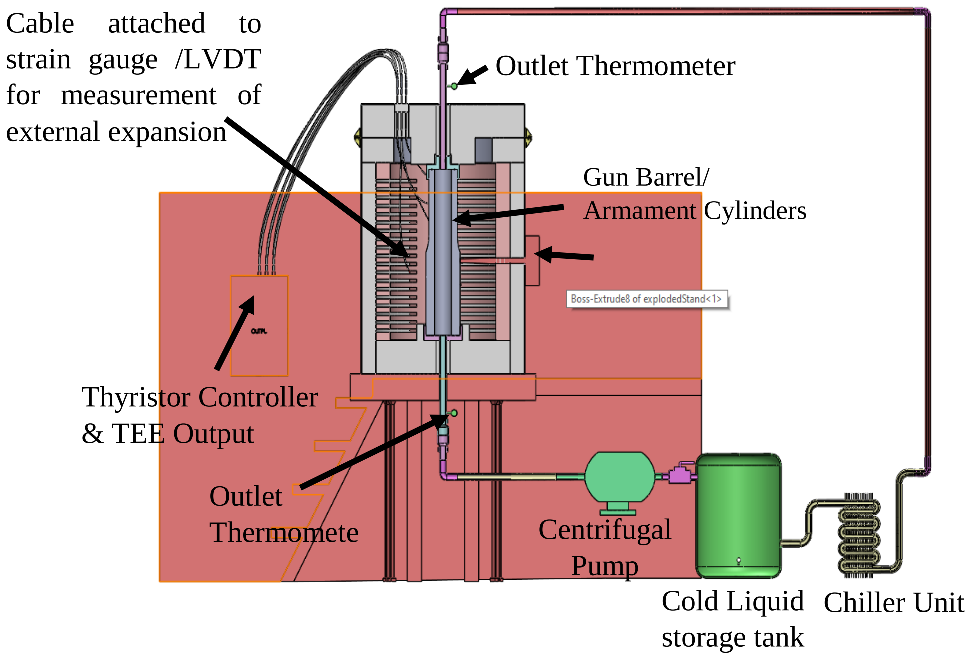

Fig. 7 CAD design layout of the modified experimental setup.

Scope of Work: Assessment of Residual Stresses in Thermally Autofrettaged ESR Barrel and Its Pressure Carrying Capacity

Milestones Achieved

- Numerical modelling of thermal autofrettage of ESR prismatic barrel incorporating actual temperature dependent material properties.
- Assessment of residual stresses and pressure carrying capacity.
- Theoretical temperature exterior expansion curve for characteristic stabilization of thermally autofrettaged barrel.

6. Numerical Estimation of Residual Stresses in ESR Barrel Induced by Thermal Autofrettage and Its Pressure Carrying Capacity

A numerical analysis of thermal autofrettage of ESR steel gun barrel is carried out considering simplest prismatic cylinder with temperature dependent mechanical properties based on the experimental evaluation. Analytically the difference of yield onset temperature between the outer and inner wall of the cylinder for thermal autofrettage was calculated as 505 ºC with the experimentally obtained data in Section 4 for cylinder with inner diameter (ID) 80 mm and outer diameter (OD) 240 mm. Thus, a temperature difference of 562 ºC between the outer and inner wall of the cylinder is considered here for achieving thermal autofrettage. To obtain the steady state temperature reached during thermal autofrettage, a model of prismatic cylinder considering the barrel material was carried out in finite element based package COMSOL. For analysis in COMSOL, a 100 kW heating source was applied on the outer diameter of the cylinder and a fluid at temperature –5 ºC was passed through the ID at 60 litres/s for thermal autofrettaging. The problem statement considered for thermal autofrettage is shown in Fig. 8.

The K-ε model was used to model the turbulent flow of cold fluid through the ID of the barrel during the process of thermal autofrettage. The conjugate heat transfer analysis was carried out during the process and the temperature of the outer wall and inner wall with time were noted. To ensure the attainment of steady state, the time at which there is no significant increase (less that 1%) in the temperatures at the OD and ID of the barrel was noted. For the present case, the computational time required to attain steady state was 2400 s. At steady state, the temperature at the OD of the cylinder was obtained as 572 ºC and that of at ID was obtained as 10 ºC. The numerical steady state temperature distribution across the wall thickness of the ESR barrel, when a temperature difference of 562 ºC is maintained between the outer and inner wall is shown in Fig. 9.

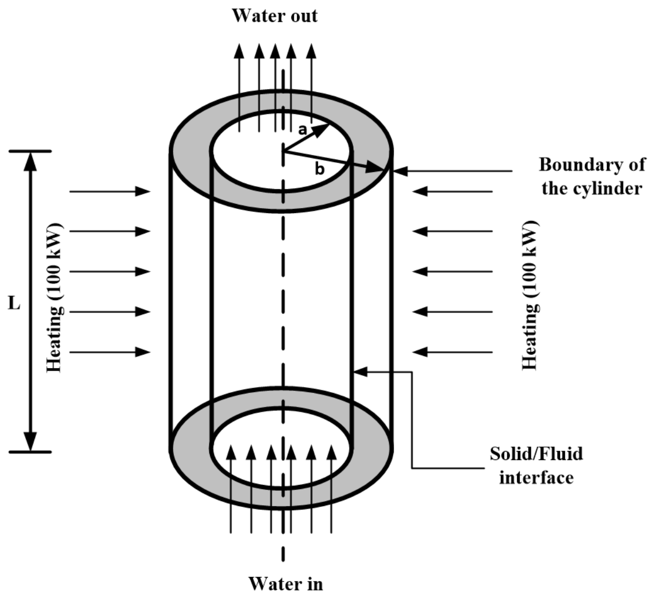

Fig. 8 Schematic representation of a prismatic ESR cylinder for the analysis of thermal autofrettage

6.1 Elastic-plastic and residual stress distribution during thermal autofrettage of ESR barrel

To assess the elastic-plastic stresses during loading and residual stresses after unloading, a coupled thermomechanical 2D generalized-plane-strain problem is solved using ABAQUS finite element package. The actual temperature dependent material properties were considered as evaluated in Section 3. The model is meshed with four-nodded generalized plane strain thermally coupled quadrilateral bilinear displacement and temperature (CPSAT) element. The displacement in the radial direction of a node at the inner boundary is restrained and a corresponding radial node at the outer boundary is fixed for the analysis. The steady state temperatures at the OD and ID of the barrel as obtained from the COMSOL finite element analysis are now imposed as Dirichlet temperature boundary conditions. The numerical elastic-plastic stress distribution obtained from the finite element analysis is shown in Fig. 10. It is observed that there is a yielding at ID as well as OD of the cylinder during loading. In thermal autofrettage yielding of the material is dictated by hoop and axial stress whereas in hydraulic autofrettage it is dictated by mainly hoop stress as axial stress is very small during hydraulic autofrettage.

The unloading step is carried out by vanishing the temperature difference, *i.e.*, cooling the barrel to room temperature. At this stage, compressive residual stresses are generated in and around the inner wall of the barrel. The residual stress distribution obtained in the barrel after unloading is shown in Fig. 11. It is observed that the residual stress obtained is compressive in nature at ID and tensile at OD of the cylinder. The residual hoop stress at ID is of the order of –267.74 MPa and residual axial stress at ID is of the order of –280.24 MPa.

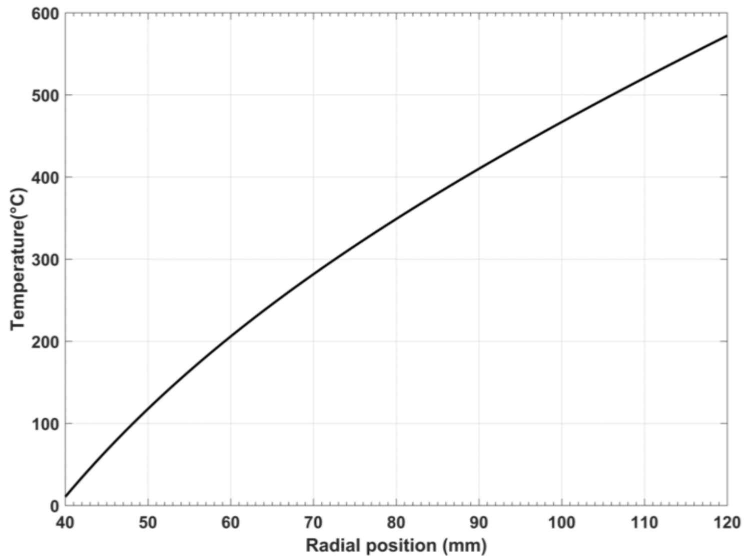

Fig. 9 Steady state temperature distribution in cylinder

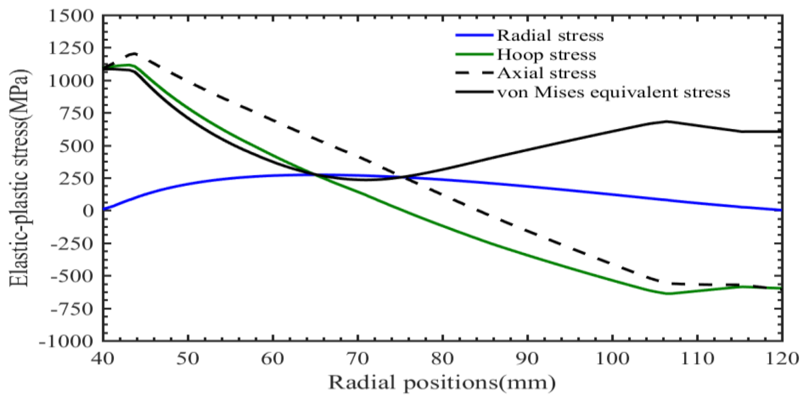

Fig. 10 Elastic-plastic stress distribution in the barrel under radial temperature difference

6.2 Numerical evaluation of pressure carrying capacity of thermally autofrettaged barrel

Due to the compressive residual stresses induced by thermal autofrettage, the barrel can take more pressure when the projectile is fired from it. The increase of pressure carrying capacity due to thermal autofrettage of the present barrel is numerically experimented and it is found the present autofrettaged barrel can withstand a pressure of 655 MPa. However, the corresponding non-autofrettaged barrel can withstand only 481.77 MPa. Thus, there is an enhancement of 38% in its pressure carrying capacity. The overall in-service stress distribution in the thermally autofrettaged barrel when subjected to 655 MPa of pressure is shown in Fig. 12.

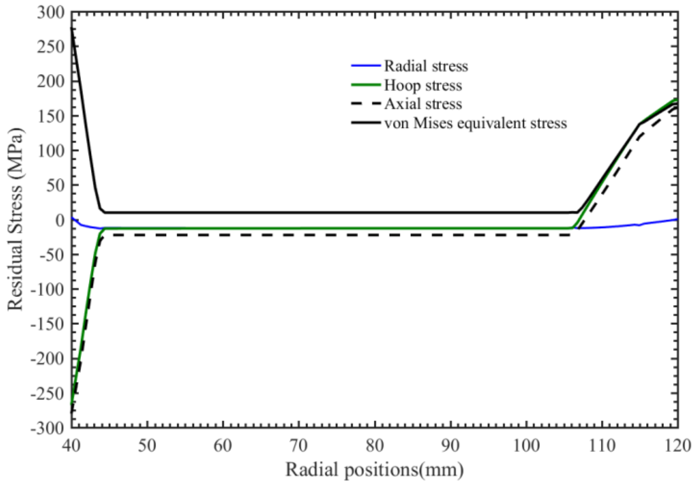

Fig. 11 Residual stress distribution in the barrel after unloading

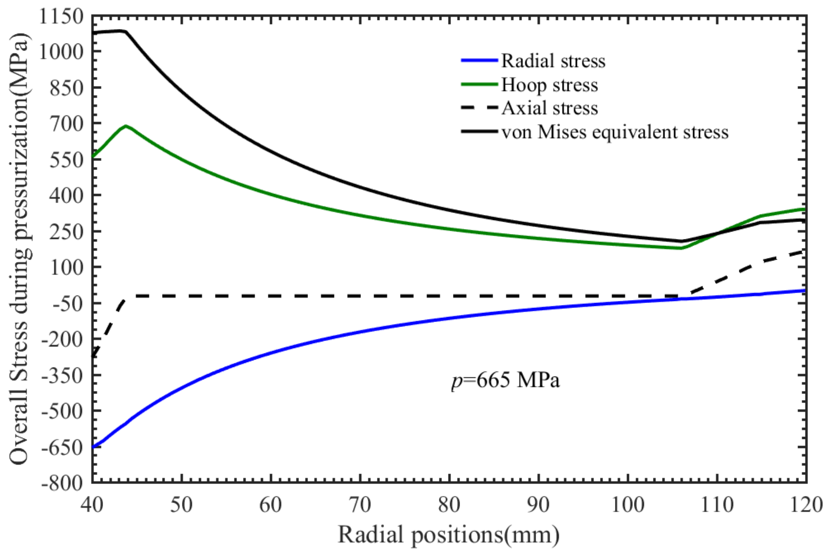

Fig. 12 Overall in-service stress distribution during internal pressurization 665 MPa.

6.3 Assessing characteristic stability of ESR barrel due to thermal autofrettage

To check the characteristics stability of the barrel material at the thermal load applied for thermal autofrettaging it becomes mandatory to apply the test temperature gradient same as thermal gradient used for thermal autofrettage. This not only checks the characteristics stability of the cylinder material but also reduces the Bauschinger effect in the cylinder. The theoretical temperature exterior expansion curve is plotted for the present case and is shown in Fig. 13. For the present barrel, there should not be difference of more than 50 μm on loaded condition and 08 μm on unloaded condition.

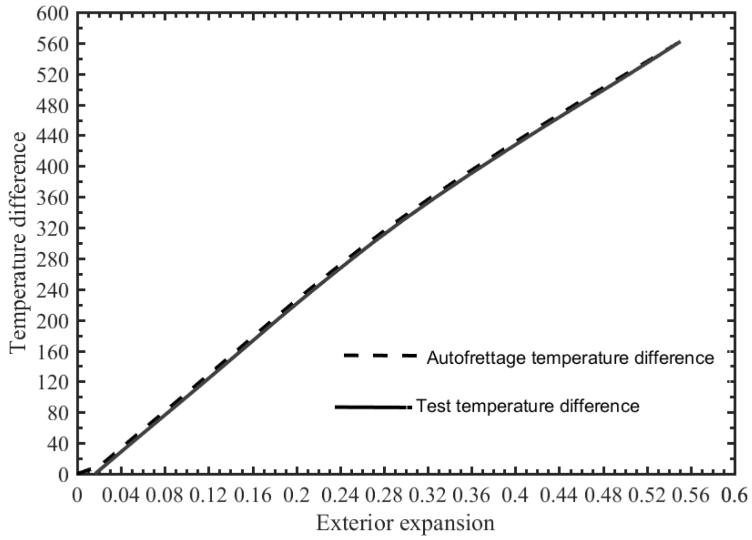

Fig. 13 Temperature exterior expansion curve for the cylinder

Scope of Work: To develop a numerical model for crack propagation in a thermally autofrettaged barrel and to experimentally determine the critical stress intensity factor K_{IC}

Milestones achieved:

In order to develop the crack propagation model, the evaluation of equivalent temperature fields in the autofrettaged cylinder is important to imitate the autofrettage induced residual stresses. In this direction, the following milestones have been achieved:

- An analytical model is developed for the equivalent temperature field to emulate the thermal autofrettage induced residual stress field.
- The equivalent temperature field is then exemplified for SS304 cylinder in a finite element framework to reproduce the original thermal autofrettage induced residual stress field.

In future, the same will be extended to ESR barrel and will be used in studying crack growth analysis using the finite element method.

7. Development of an Analytical Model for the Equivalent Temperature Field to Imitate the Thermal Autofrettage Induced Residual Stress Field in Cylinders

In this section, a methodology for emulating the residual stress field in a long thick-walled cylinder induced by thermal autofrettage is developed by establishing equivalence between the thermal stress field and the thermal autofrettage analytical or numerical residual stress fields. A closed-form analytical model is developed for evaluating the equivalent temperature field that reproduces the residual stress field in a cylinder subjected to thermal autofrettage using Kamal and Dixit's model [4]. The developed analytical model is numerically exemplified for a typical thermally autofrettaged cylinder by performing FEM analysis. This involves applying the equivalent temperature fields evaluated from the analytical model to the hollow cylinder in ABAQUS finite element framework and reproducing the corresponding residual stresses as originally induced by thermal autofrettage.

7.1 Mechanics of Thermal Autofrettage

For emulating the thermal autofrettage induced residual stress field by means of equivalent temperature field, it is important to understand the mechanics of thermal autofrettage. Here, the mechanics of thermal autofrettage developed by Kamal and Dixit [4] is briefly described.

In a thick-walled long cylinder with free ends under radial temperature gradient, the steady-state temperature distribution is given by Eq. (15). When the cylinder is loaded with a radial temperature difference, there are three situations of deformation occurring in the wall of the cylinder. The cylinder wall remains elastic if the temperature difference is below a certain first threshold, which is the yield onset temperature difference of the cylinder. Once it exceeds the first threshold temperature difference as per Tresca criterion, the inner wall of the cylinder is subjected to plastic deformation two consecutive plastic zones, *viz*., $a \leq r \leq c$ and $c \leq r \leq d$. The zone, $d \leq r \leq b$ at the outer portion of the cylinder wall deforms elastically. This situation of deformation is referred as the first stage of plastic deformation as depicted in Fig. 14 (a). Further, if the temperature difference is allowed to reach a certain second threshold, yielding initiates at the outer wall of the cylinder as well. Upon exceeding the second threshold temperature difference, the cylinder wall is formed with two more consecutive plastic zones propagating radially inwards from the outer wall, *viz*., $f \leq r \leq b$ and $e \leq r \leq f$ apart from the two inner plastic zones formed in the first stage of plastic deformation. The intermediate zone, $d \leq r \leq e$ remains in the elastic state. This situation of deformation is referred as the second stage of plastic deformation as shown in Fig. 14 (b). The radii *d* and *e* are called as the elastic-plastic interface radii. In a later stage, when the temperature difference is vanished by cooling the cylinder to room temperature, beneficial compressive residual stresses are set up at the inner side of the cylinder along with tensile residual stresses towards the outer wall of the cylinder. The detailed derivation of the thermal stresses induced in the cylinder when loaded with a plastically deforming temperature difference as well as the post-unloading residual stresses induced in the first and second stage of plastic deformation can be found in Ref [4]. The analysis is based on generalized plane strain condition, Tresca yield criterion and its associated flow rule.

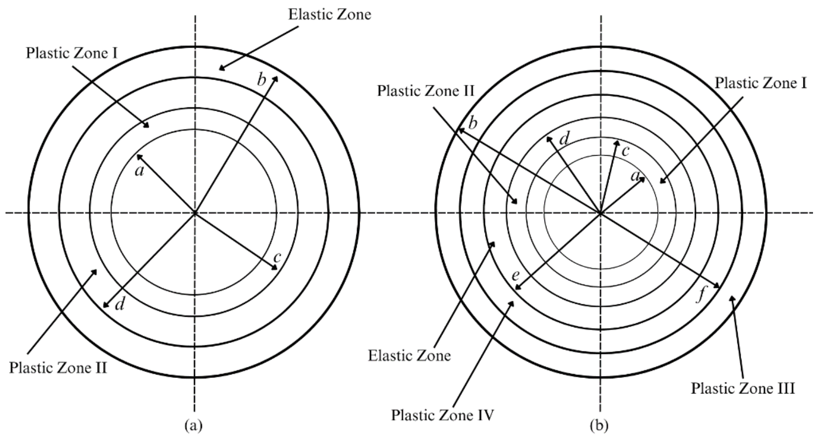

Fig. 14 (a) First and (b) second stage of plastic deformation with different plastic and elastic zones in thermally autofrettaged cylinder [4]

7.2 The Equivalent Temperature Field

In an axisymmetric hollow cylinder with inner radius *a* and outer radius *b*, the states of elastic stress due to generalized plane strain condition under steady state temperature field $T(r)$ are given by [9]

$$\sigma_{rr}(r) = -\frac{\alpha E}{(1-\nu)}\left(\frac{1}{r^2}\right)\int_a^r T(r)r\mathrm{d}r + \frac{E}{(1+\nu)}\left\{\frac{M}{(1-2\nu)} - \frac{N}{r^2}\right\}, \quad (28)$$

$$\sigma_{\theta\theta}(r) = \frac{\alpha E}{(1-\nu)}\left(\frac{1}{r^2}\right)\int_a^r T(r)r\mathrm{d}r - \frac{\alpha E T(r)}{(1-\nu)} + \frac{E}{1+\nu}\left\{\frac{M}{(1-2\nu)} + \frac{N}{r^2}\right\}, \quad (29)$$

where *M* and *N* are integration constants. Using the boundary conditions of vanishing radial stress at $r = a$ and $r = b$, the integration constants *M* and *N* can be evaluated by using the following boundary conditions:

$$\left(\sigma_r\right)\Big|_{r=a} = 0, \tag{30}$$

$$\left(\sigma_r\right)\Big|_{r=b} = 0. \tag{31}$$

Using Eqs. (30) and (31) and solving the resulting equations, the constants *M* and *N* are obtained as

$$M = \frac{\alpha\left(1+\nu\right)\left(1-2\nu\right)}{\left(1-\nu\right)\left(b^2-a^2\right)}\int_a^b T\left(r\right) r\mathrm{d}r, \tag{32}$$

$$N = \alpha\left(\frac{1+\nu}{1-\nu}\right)\frac{a^2}{b^2-a^2}\int_a^b T\left(r\right) r\mathrm{d}r. \tag{33}$$

Substituting Eqs. (32) and (33) in Eqs. (28) and (29), the resulting radial and hoop stress distribution as a function of temperature is obtained as

$$\sigma_{rr}(r) = \left(\frac{1}{1-\nu}\right)\frac{E\alpha}{r^2}\left\{\frac{r^2-a^2}{b^2-a^2}\int_a^b T(r) r\mathrm{d}r - \int_a^r T(r) r\mathrm{d}r\right\}, \tag{34}$$

$$\sigma_{\theta\theta}(r) = \left(\frac{1}{1-\nu}\right)\frac{E\alpha}{r^2}\left\{\frac{r^2+a^2}{b^2-a^2}\int_a^b T(r) r\mathrm{d}r + \int_a^r T(r) r\mathrm{d}r - T(r) r^2\right\}. \tag{35}$$

To evaluate the hoop stress at inner radius $r = a$, Eq. (35) can be rewritten in the following form providing definite integral as:

$$I_1 = \int_a^b T(r) r\mathrm{d}r = \sigma_{\theta\theta}(a)\left(\frac{b^2-a^2}{2}\right)\left(\frac{1-\nu}{E\alpha}\right) + \left(\frac{b^2-a^2}{2}\right) T(a)\,. \tag{36}$$

Adding Eqs. (34) and (35) yields

$$I_1 = (1-\nu)\left(\frac{b^2-a^2}{2}\right)\frac{\sigma_{rr}(r)+\sigma_{\theta\theta}(r)}{E\alpha} + \left(\frac{b^2-a^2}{2}\right) T(r)\,. \tag{37}$$

Comparing Eq. (36) with Eq. (37), the temperature field as a function of radial position is obtained as

$$T(r_i) = \left(\frac{1-\nu}{E\alpha}\right)\left\{\sigma_{\theta\theta}(a) - \sigma_{rr}(r_i) - \sigma_{\theta\theta}(r_i)\right\} + T(a)\,. \tag{38}$$

The analytical equivalent temperature field can be determined using Eq. (38) by substituting the distributions of residual thermal stress resulting from thermal autofrettage, $\sigma_{rr}(r_i)$ and $\sigma_{\theta\theta}(r_i)$. The equivalent temperature field so obtained can exactly replicate the residual stress distribution due to thermal autofrettage in cylinder. This amounts to an inverse estimation of the temperature field that causes a prior stress field.

7.2.1 Analytical solutions for the equivalent temperature field for a thermally autofrettaged cylinder subjected to first stage of plastic deformation

A cylinder subjected to thermal autofrettage undergoing first stage of plastic deformation is considered. The three zones, *viz*. plastic zone I, plastic zone II and elastic zone commences when the temperature difference crosses the first threshold as depicted in Fig. 14(a). In this case, the analytical solutions for the equivalent temperature field in different zones can be obtained by substituting the respective residual stress distributions in Eq. (38) either from analytical solutions or numerical discrete solutions.

Here, as an example, using the residual stress distributions from Kamal and Dixit [4] for first stage of plastic deformation, in Eq. (38), the solution for equivalent temperature field in the Plastic zone I, II and in the outer elastic zone are obtained as

Plastic zone I, $a \le r \le c$:

$$T(r) = \left(\frac{1-\nu}{E\alpha}\right)\left\{k_1\sigma_Y \ln\left(\frac{a}{r^2}\right) + \frac{E\alpha\left(T_b - T_a\right)}{1-\upsilon}\frac{\ln\left(\frac{a}{r}\right)}{\ln\left(\frac{b}{a}\right)} - C_3\right\} + T_a. \tag{39}$$

Plastic zone II, $c \le r \le d$:

$$T(r) = \left(\frac{1-\nu}{E\alpha}\right)\left[\begin{array}{l} k_1\sigma_Y\left\{1+\ln(a) - \left(\frac{2}{2\nu-1}\right)\right\} + C_3 - \frac{E\alpha\left(T_b-T_a\right)}{(1-\nu)\ln\left(\frac{b}{a}\right)}\ln\left(\frac{r}{a}\right) - C_5\left\{r^{\sqrt{2(1-\nu)}-1}\left(\sqrt{2(1-\nu)}+1\right)\right\} \\ -C_6\left\{r^{-\sqrt{2(1-\nu)}-1}\left(1-\sqrt{2(1-\nu)}\right)\right\} - \frac{2E\alpha T_a}{(2\nu-1)} - \frac{E\alpha\left(T_b-T_a\right)}{(2\nu-1)\ln\left(\frac{b}{a}\right)}\left\{\begin{array}{l} 2\ln\left(\frac{r}{a}\right) - \\ \frac{3+2\nu}{2\upsilon-1}\end{array}\right\} + \frac{2E\varepsilon_o}{(2\nu-1)} \end{array}\right] + T_a. \tag{40}$$

Elastic zone, $d \le r \le b$:

$$T(r)=\left(\frac{1-\nu}{E\alpha}\right)\left[\begin{array}{l} k_1\sigma_Y\left\{1+\ln\left(a\right)\right\}+C_3 \\ +\dfrac{E\alpha\left(T_b-T_a\right)}{2\left(1-\nu\right)\ln\left(\dfrac{b}{a}\right)}\left\{\begin{array}{l} 1-2\ln\left(\dfrac{b}{a}\right)+2\left\{\dfrac{d^2}{b^2+d^2\left(2\nu-1\right)}\right\} \\ \left\{\ln\left(\dfrac{b}{a}\right)\left(2\nu-1\right)-\nu-\ln\left(\dfrac{d}{a}\right)\right\} \end{array}\right\} \\ -\left\{\dfrac{2d^2}{b^2+d^2\left(2\nu-1\right)}\right\}\left(k_1\sigma_Y+E\alpha T_a-E\varepsilon_o\right) \end{array}\right]+T_a. \quad (41)$$

7.2.2 Analytical solutions for the equivalent temperature field for a thermally autofrettaged cylinder subjected to second stage of plastic deformation

During the second stage of plastic deformation in thermal autofrettage, there exists two additional plastic zones, Plastic zone III, $f \le r \le b$ and Plastic zone IV, $e \le r \le f$ at the outer wall of the cylinder with an intermediate zone, $d \le r \le e$ as depicted in Fig. 14 (b). Using the respective residual stress equations from Kamal and Dixit [4], the analytical equivalent temperature field for replicating the original autofrettage induced residual stress distribution in the two outer plastic zones and in the intermediate elastic zone for the second stage of plastic deformation are obtained as follows:

Plastic zone III, $f \le r \le b$:

$$T(r)=\left(\frac{1-\nu}{E\alpha}\right)\left[\begin{array}{l} k_1\sigma_Y\left(2+2\ln r+\ln a\right)+C_3-2C_7 \\ -\dfrac{E\alpha(T_b-T_a)}{(1-\nu)\ln\left(\dfrac{b}{a}\right)}\ln\left(\dfrac{r}{a}\right) \end{array}\right]+T_a \quad (42)$$

Plastic zone IV, $e \le r \le f$:

$$T(r) = \left(\frac{1-\nu}{E\alpha}\right) \left[\begin{array}{l} k_1\sigma_Y \left\{ 1 + \ln(a) - \frac{2}{(2\nu-1)}\left(1+\frac{e^2}{2d^2}\right) + 2\ln\left(\frac{r}{e}\right) \right\} + C_3 \\ -\frac{E\alpha(T_b - T_a)}{2(1-\nu)\ln\left(\frac{b}{a}\right)} \left[\frac{2}{(2\nu-1)} \left\{ \ln\left(\frac{d}{a}\right) + \frac{1}{2} - \frac{e^2}{2d^2} \right\} + 2\ln\left(\frac{r}{e}\right) \right] \\ -\frac{2E\alpha T_a}{(2\nu-1)} - \frac{2E\varepsilon_o}{(1-2\nu)} \end{array} \right] + T_a \tag{43}$$

Elastic zone, $d \le r \le e$:

$$T(r) = \left(\frac{1-\nu}{E\alpha}\right) \left[\begin{array}{l} k_1\sigma_Y \left\{ 1 + \ln(a) \right\} + C_3 - \frac{2E\alpha T_a}{(2\nu-1)} \\ -\frac{E\alpha(T_b - T_a)}{2(1-\nu)\ln\left(\frac{b}{a}\right)} \left\{ \frac{2}{(2\nu-1)} \left\{ \ln\left(\frac{d}{a}\right) + \frac{1}{2} - \frac{e^2}{2d^2} \right\} \right\} \\ -\frac{2k_1\sigma_Y}{(2\nu-1)}\left(1+\frac{e^2}{2d^2}\right) - \frac{2E\varepsilon_o}{(1-2\nu)} \end{array} \right] + T_a \tag{44}$$

The analytical equivalent temperature fields in the Plastic zone I and II during second stage of plastic deformation is still given by Eqs. (39) and (40), where the values of the constants are different due to change of boundary conditions. The different constants exist in the equations presented in Sections 7.2.1 and 7.2.2 are readily available in Kamal and Dixit [4].

7.3 Numerical Exemplification of the Equivalent Temperature Field in Thermal Autofrettage of SS304 Cylinder

To exemplify the analytical model developed in Section 7.2 for the equivalent temperature field to imitate the original thermal autofrettage induced residual stress field in cylinder, an SS304 cylinder with the following radial dimensions is considered: inner radius *a*=10 mm and outer radius *b*=30 mm. The material properties of SS304 are presented in Table 6. To achieve thermal autofrettage in the current SS304 cylinder, the different geometrical and loading parameters as obtained in Ref [4] are taken and summarized in Table 7.

Table 6 Material Properties of SS304

Density, ρ (kg/m^3)	Young's Modulus of Elasticity, E (GPa)	Poisson's ratio, ν	Yield stress, σ_Y (MPa)	Coefficient of thermal expansion, α (/ °C)
8000	193	0.30	205	17.2×10^{-6}

Table 7 Geometry and loading parameters in the thermal autofrettage of SS304 cylinder [4]

Radius of plastic-plastic interface, c (mm)	Radius of elastic-plastic interface, d (mm)	Temperature at the inner wall, T_a (°C)	Autofrettage temperature difference, $(T_b - T_a)$ (°C)
11.9775	12.9193	25	120

7.3.1 Evaluation of equivalent temperature field

For the present autofrettage temperature difference induced in the SS304 cylinder, the cylinder is subjected to first stage of plastic deformation during thermal autofrettage. Thus, the equivalent temperature field in the cylinder in the two consecutive inner plastic zones and in the outer elastic zone are evaluated using equations presented in Section 7.2.1. The distribution of the equivalent temperature field for imitating the residual stress field in the thermally autofrettaged SS304 cylinder as a function of radius is shown in Fig. 15. It is observed that the equivalent temperature field decreases up to the radius of elastic-plastic interface d and then it becomes constant in the elastic zone.

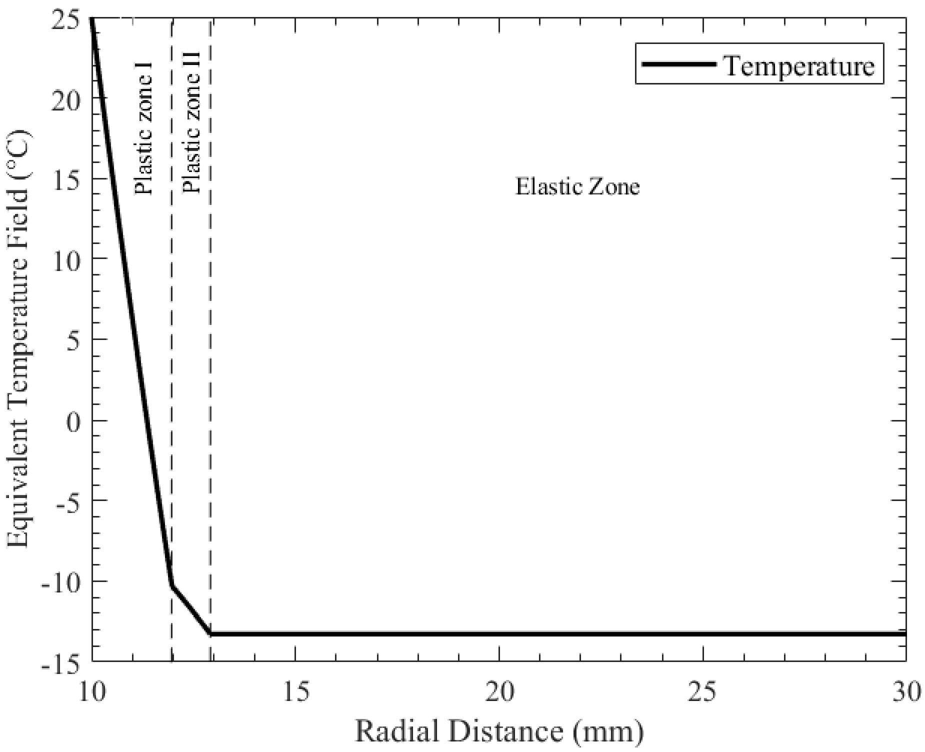

Fig. 15 The equivalent temperature field for imitating the original residual stresses induced by thermal autofrettage in SS304 Cylinder

7.3.2 Corroboration of the residual stress field induced by the equivalent temperature in the FEM model with the original thermal autofrettage induced residual stresses

In this section, the residual stress distribution in the SS304 cylinder is evaluated by applying the equivalent temperature field obtained in Section 7.3.1 in a two-dimensional finite element method (FEM) model and are corroborated with the original thermal autofrettage induced residual stress field due to Kamal and Dixit's model [4]. The FEM modelling is carried out using ABAQUS finite element package.

For the FEM analysis, the cross section of the cylinder with inner and outer radii 10 mm and 30 mm respectively is considered with the centre at the origin of a polar coordinate system. The geometry is meshed by using CPEG4R 4-noded bilinear generalized plane strain element of size 0.2 mm. A typical meshed geometry is shown in Fig 16. The meshing was done using sweep method. The number of nodes and elements used in the present model are 63226 and 62600, respectively. The equivalent temperature field obtained from Fig. 15 were applied on each and every radial node corresponding to each radial distance. The displacement boundary conditions were imposed to solve the FEM model. The displacement in the r-direction at a node in the inner radius is constrained (u_r=0) and a node at the outer boundary of the cylindrical cross-section is fixed, *i.e.*, the displacements of the node both in the r and θ-directions are fixed (u_r=0, u_θ=0). The FEM model is then solved to obtain the radial, hoop and axial stress distributions.

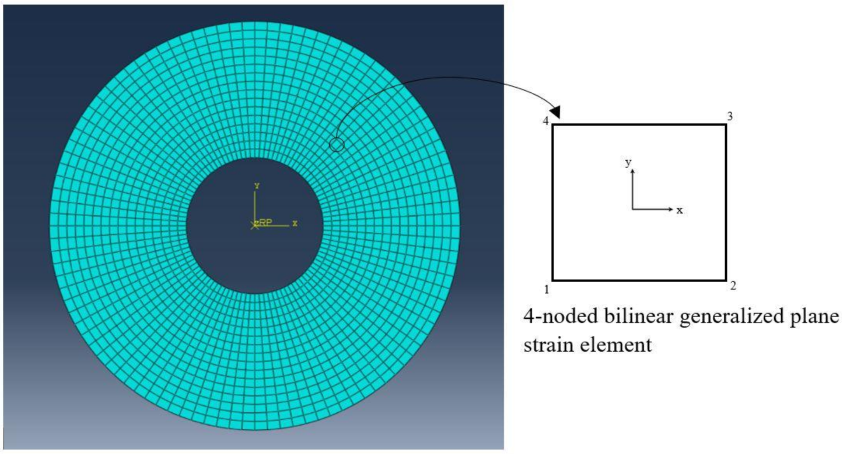

Fig. 16 A typical meshed geometry

The FEM stress solutions obtained by incorporating the equivalent temperature field are corroborated with the residual stress field originally induced by the method of thermal autofrettage using the solutions of Kamal and Dixit [4]. The corroboration of equivalent temperature field generated residual radial, hoop and axial stresses with the original thermal autofrettage induced residual stresses are shown in Figs. 17 (a), (b) and (c), respectively. It is observed that all the components of the residual stress fields obtained from FEM model is matching well with the original analytical generalized plane strain thermal autofrettage residual stress field. Thus, the analytical model for the equivalent temperature field developed in Section 7.2 is capable of reproducing the residual stress field induced by thermal autofrettage in cylinders with reasonable accuracy.

The methodology presented here for SS304 as an example. In future, it will be used for ESR gun barrel and will be utilized in studying the crack propagation in a thermally autofrettaged barrel.

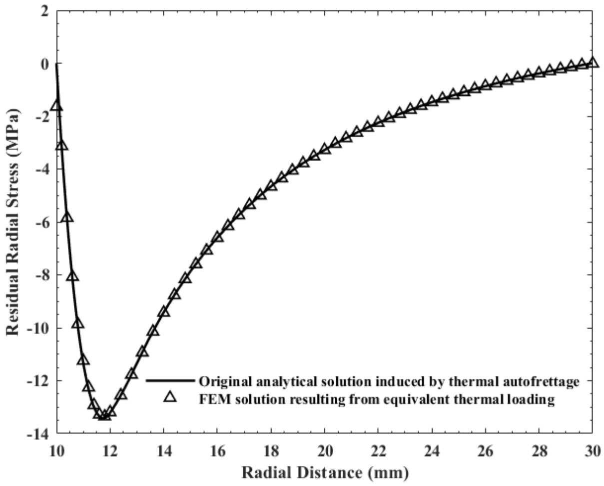

(a)

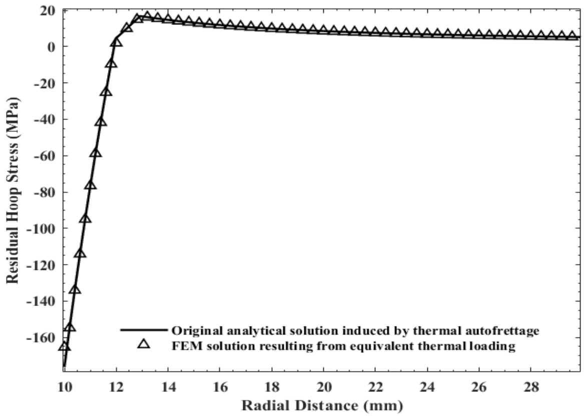

(b)

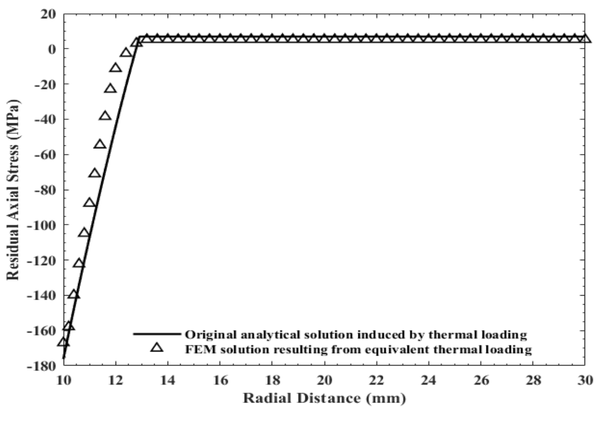

(c)

Fig. 17 Comparison of residual (a) radial, (b) hoop and (c) axial stress in the thermal autofrettage resulting from analytical solutions and present FEM solution due to equivalent temperature field

8. Reason for Short Closure of the Project

While the preliminary experimental as well as numerical works towards achieving the proposed objectives of the project was in progress as detailed in this report, an unforeseen situation of additional equipment was aroused. The additional equipment required are an electric pit furnace of 100 kW capacity and a chiller unit as described in Section 5. It is to be noted here that the new requirement of an electric pit furnace with control unit and a chiller unit was placed before the ADMB panel and based on the recommendation of the panel the tendering for purchase of pit furnace was exercised. The technical bid as well as financial bid for the received tenders were evaluated and finally based on L1, one suitable vendor was selected. However, there was not enough fund under equipment head of the project, it could not be procured on time. As a consequence, the requirement of additional fund under equipment head with justification was placed in the 23rd ADMB panel meeting held on Sep 9, 2022 and the panel recommended for the same. On Oct 27, 2022 a meeting was also held through video conferencing with the Member Secretary, ARMREB along with the user lab scientist and ADMB panel coordinator to discuss about the status of the additional fund requirement under equipment head. The member Secretary told that the matter of additional fund requirement by the PI is under consideration. Meanwhile, some numerical works related to the project was in progress and suddenly, on Feb 17, 2023, the PI received an email from the Member Secretary, ARMREB stating that the request for additional fund requirement has not been recommended and requested to stop all financial transaction till further decision is communicated. After that in the ADMB panel meeting held on March 25, 2023, the Member Secretary, ARMREB informed the panel that although the additional fund requirement was recommended by the panel for the project, but it has not been approved by the competent authority. In view of this, the panel recommends for short closure of the project. If required, the panel also suggested that a new project can be proposed to complete the added and additional objectives of the project.

9. Conclusions

The project was aimed to study the feasibility of a new thermal autofrettage method for strengthening gun barrel considering actual temperature dependent material properties. There were total five scopes of work were identified for the current project. These are

i. To develop an experimental setup for an innovative thermal autofrettage process for gun barrel.

ii. To assess residual stresses, pressure carrying capacity, material properties and microstructural characterization of thermally autofrettaged cylinder/barrel.
iii. To relieve tensile residual stresses in the thermally autofrettage tube.
iv. To measure dimensional changes and bore straightness in the thermally autofrettaged cylinder/barrel.
v. To develop a numerical model for crack propagation in a thermally autofrettaged barrel and to experimentally determine the critical stress intensity factor K_{IC}.

Out of the above scopes, certain milestones have been achieved towards completion of the Scopes (i), (ii) and (v) partially. All the milestones achieved are presented in this report. However, as the project comes to a short closure due to financial crunch in procuring the required equipment as stated in Section 8, all the scopes could not be completed. As per the recommendation of the panel meeting held on March 25, 2023, a fresh proposal will be submitted to ARMREB, DRDO, where the incomplete scopes along with some new scopes will be included. As the process of thermal autofrettage is a new one adding certain edge over the practicing hydraulic autofrettage, the process needs to be established as a potential industrial process. The PI and Co-PI of this project are keen to achieve this milestone for the Indian Defence sector. The thermal autofrettaging is one of the potential alternative autofrettaging process, which can be used for all types of metallic cylinders used in armament, *e.g.*, recoil cylinder, equilibrator cylinder etc.

References

[1] Jacob, L., La Résistance et L'équilibre Elastique des Tubes Frettés, Mémoire de L'artillerie Navale, 1907, 1(5), pp. 43–155 (in French).

[2] Avitzur, B. Autofrettage–stress distribution under load and retained stresses after depressurization, International Journal of Pressure Vessel and Piping, 1994, 57, pp. 271–287.

[3] Davidson, T.E., Barton, C.S., Reiner, A.N. and Kendall, D.P., New approach to the autofrettage of high-strength cylinders, Experimental Mechanics, 1962, 2, pp. 33–40.

[4] Kamal S.M. and Dixit U.S., Feasibility study of thermal autofrettage of thick-walled cylinders, ASME Journal of Pressure Vessel Technology, 2015, 137(6), pp. 061207-1−061207-18.

[5] Kamal S.M., Borsaikia A.C. and Dixit U.S., Experimental assessment of residual stresses induced by the thermal autofrettage of thick- walled cylinders, Journal of Strain Analysis for Engineering Design, 2016,51(2), pp. 144–160.

[6] Kamal S.M., Dixit U.S., Roy A., Liu Q. and Silberschmidt V.V., Comparison of plane-stress, generalized-plane- strain and 3D FEM elastic-plastic analyses of thick-walled cylinders subjected to radial thermal gradient, International Journal of Mechanical Sciences,2017,131-132, pp. 744−752.

[7] Kamal S.M. and Dixit U.S., A comparative study of thermal and hydraulic autofrettage, Journal of Mechanical Science and Technology, 2016, 30(6), pp. 2483−2496.

[8] Kamal S.M. and Dixit U.S., A study on enhancing the performance of thermally autofrettaged cylinder through shrink-fitting, ASME Journal of Manufacturing Science and Engineering, 2016, 138(9), pp. 094501-1−094501-5.

[9] Timoshenko S.P. and Goodier J.N., Theory of Elasticity, 3rd ed., McGraw-Hill, New York, 1970.

Certificate for Completion of Work

It is certified that all the approved objectives of the project **ARMREB/ADMB/2021/234** have been achieved fully. Nevertheless, some of the objectives are partially achieved as summarized in Table 1 below

Table 1

Approved Objectives	Outcome
To develop an experimental setup for an innovative thermal autofrettage process for gun barrels	Only the layout of the thermal autofrettage system was designed. Further, for the purpose of experimentation, the temperature dependent thermo-mechanical properties of the actual gun barrel material (ESR) were determined experimentally.
To assess residual stresses, pressure carrying capacity, material properties and microstructural characterization of thermally autofrettaged cylinders/barrels.	Partially achieved through numerical simulation.
To relieve tensile residual stresses in the thermally autofrettage tube	**Not achieved.**
To measure dimensional changes and bore straightness in the thermally autofrettaged cylinder/barrel.	**Not achieved.**
To develop a numerical model for crack propagation in a thermally autofrettaged barrel and to experimentally determine the critical stress intensity factor K_{IC}	The development of numerical model was initiated. As a first step, an analytical model for the equivalent temperature field to reproduce the original residual stress field in the cylinders due to thermal autofrettage has been developed.

31/7/2023

Principal Investigator

Executive Summary of Project

1. Title of Project – Use of Thermal Autofrettage for Defence Application

2. Name of the Principal Investigator – Dr. Seikh Mustafa Kamal

3. Name of the Institution – Tezpur University

4. Cost of the Project – Rs 41, 33,726/-

5. Date of Sanction – 14 June 2021, (Amended 21 Sep 2021)

6. Date of Completion – 25 March 2023

7. Aim of the Project –

- To develop an experimental setup for an innovative thermal autofrettage process for gun barrel.
- To assess residual stresses, pressure carrying capacity, material properties and microstructural characterization of thermally autofrettaged cylinders/barrels.
- To relieve tensile residual stresses in the thermally autofrettage tube
- To measure dimensional changes and bore straightness in the thermally autofrettaged cylinder/barrel.
- To develop a numerical model for crack propagation in a thermally autofrettaged barrel and to experimentally determine the critical stress intensity factor K_{IC}

8. Requirement Envisaged – The requirement envisaged in addition to the sanctioned amount was supposed to be provided by the funding agency itself.

9. Achievement – a) Experimental determination of temperature dependent material properties of actual gun barrel material.

b) An analytical model to determine the yield onset temperature difference for ESR barrel.

c) The layout of the thermal autofrettage system for gun barrel was designed.

d) Numerical analysis of the thermal autofrettage system.

e) Development of an analytical model for equivalent temperature field to replicate the thermal autofrettage induced residual stresses in cylinders.

10. Likely application of outcome – For strengthening gun barrels and other high pressure vessels.

11. Likely end use – Application in high caliber gun barrels to increase the pressure carrying capacity and fatigue life as an alternative to the hydraulic/swage autofrettage.

12. Details of Equipment acquired under project – Workstation (for numerical analysis)

13. No. of Research staff engaged under the project – 01

14. No. of student/researchers benefited under the project – 01 PhD (Ongoing), 01 M.Tech (completed) and 03 B.Tech (completed) benefitted by the project

15. No. of paper published in National Conference with Impact factor –

16. No. of papers published in International Conference with Impact factor – 01

17. No. of papers published in International Journal with Impact factor – Two papers are under preparation. The details are as follows:

a) Roy, A.K., Kamal, S.M., Patil, R.U., Bora, P., and Rao, V.V., Numerical Analysis of Thermal Autofrettage Process for Smoothbore Gun Barrel Considering Actual Material Properties.

b) Roy, A.K., Kamal, S.M., Patil, R.U., Rao, V.V., Sharmah, Indranuj, Swargiary, K. and Lahe, J.P., Determination of Equivalent Temperature Field for Imitating the Thermal Autofrettage Induced Residual Stress Field in Cylinders.

18. No. of thesis for PhD/ M. Tech realized under the project with details –

Details of PhD

Sl. No.	Name of the student/ research scholar	Title of the thesis	Doctorate / Master's level	Year of completion (or in progress)
1.	Mr. Arun Roy	A Numerical and experimental Analysis of residual stresses in thermal autofrettage of gun barrels	Doctorate	In progress

Details of M.Tech

Sl. No.	Name of the student/ research scholar	Title of the thesis	Doctorate / Master's level	Year of completion (or in progress)
1.	Debojit Buragohain	Numerical Simulation of a Thermal Autofrettage System	Master's	2023

Details of B.Tech

Sl. No.	Name of the student/ research scholar	Title of the thesis	Bachelor's Degree	Year of completion (or in progress)
1	Indranuj Sharma Jyotish Prasad Lahe Ketupati Swargiary	Development of an Analytical Model for the Equivalent Temperature Field to Imitate the Thermal Autofrettage Induced Residual Stress Field in Cylinders	B.Tech	2023

19. No. of Patents development/ sealed under the project – None

20. Steps taken by PI for dissemination of research work- None

21. Suggestion, if any for future research work

In the present research project, it was proposed to develop an experimental set up for the thermal autofrettage of gun barrels. In this project, only an experimental set up of thermal autofrettage for gun barrel was conceived and CAD modeling of the system layout was accomplished. The set up could not materialize due to the involvement of costly equipment, which was not anticipated at the time of original submission of the project. Thus, there was a requirement of additional fund above the sanctioned amount for procuring equipment needed for the set up. The matter of fund enhancement was proposed in one of the panel meeting and accordingly panel recommended for the same. However, the competent authority did not sanction the additional fund required for the project. Based on this, the ARMREB, ADMB Panel recommended for the short closure of the project and suggested for submitting a fresh proposal to address the remaining objectives of this current project. Thus, the future research involves the setting up of a thermal autofrettage system for gun barrel and various other aspects as follows:

a) Rigorous numerical estimation of residual stresses in thermal autofrettage of a gun barrel and analysis of its beneficial effects, *viz.*, pressure carrying capacity and fatigue life.
b) Design and development of an experimental setup for thermal autofrettage of a monobloc gun barrel and experimentally validate the numerical results.
c) To develop a numerical model for assessment of the effect of thermal autofrettaging, and experimental validation of the same (e.g., thermal exterior expansion (TEE) Curve, difference in exterior expansion for thermal gradient for thermal autofrettage and thermal gradient for test for thermal autofrettage for characteristic stability of the barrel material, etc.).
d) Comparative study of effects of thermal autofrettage hydraulic autofrettage for a monobloc gun barrel.
e) To study the effect of thermal autofrettaging combined with shrink-fit.

22/8/2023

(Signature with official seal)

(Principal Investigator)

Assistant Professor
Dept. of Mechanical Engg.
Tezpur University

Kalita
22/08/2023

(Signature with official seal)

(Head of Department)

Head
Dept. of Mechanical Engg.
Tezpur University

AUDITED/ PROVISIONAL STATEMENT OF EPENDITURE ACCOUNTS

For the Financial Year (15/11/2021 to 31/3/2022)

a. Title of the Project: Use of Thermal Autofrettage for Defence Application

b. Sanctioned letter no. & date: ARMREB/ADMB/2021/234 & 14 June 2021 (Amendment dated 21 Sep 2021)

c. Principal Investigator: Dr. Seikh Mustafa Kamal

d. Date of start of the project: 15 November, 2021

e. Total sanctioned cost of the project in Rs: 41,33,726/-

f. Grant received (Rs.) in I yr 24,96,682/- **II yr** NIL **III yr** NIL

g. Total grants received so far: Rs. 24,96,682/-

S. No	Sanctioned Heads	Funds sanctioned for the year Rs.	Funds released Rs.	Carried forward from previous year Rs.	Funds available (iv+v) Rs.	Expenditure incurred during the FY Rs.	Balance (vi-vii) Rs.	Commitments Rs.	Total expenditure (vii+ix) Rs.
i	ii	iii	iv	v	vi	vii	viii	ix	x
(a)	Staff	4,31,520	4,31,520	NIL	4,31,520	42,313	3,89,207	NIL	42,313
(b)	Equipment	16,70,000	16,70,000	NIL	16,70,000	79,744	15,90,256	NIL	79,744
(c)	Operation & Maint.	NA	NA	NA		NA	NA	NA	NA
(d)	Expendables	1,35,000	1,35,000	NIL	1,35,000	NIL	1,35,000	NIL	NIL
(e)	Travel	50,000	50,000	NIL	50,000	38,469	11,531	NIL	38,469
(f)	Contingencies	35,000	35,000	NIL	35,000	2,500	32,500	NIL	2,500
(g)	Research Consultant	NA	NA	NA	NA	NA	NA	NA	NA
(h)	Procured Service	NA	NA	NA	NA	NA	NA	NA	NA
	Institutional over head	1,75,162	1,75,162	NIL	1,75,162	1,09,476	65,686	NA	1,09,476
	Interest earned, if any				20,852		20,852		
	TOTAL	24,96,682	24,96,682	NIL	25,17,534	2,72,502	22,45,032	NIL	2,72,502

(Dr. SEIKH MUSTAFA KAMAL)
Name and Signature of
Principal Investigator
Date: 31/7/2023

Name and Signature of
Accounts Officer
Date:
Finance Officer
Tezpur University

Signature of Administrative
Date:
Registrar
Tezpur University

UTILIZATION CERTIFICATE

FOR THE FINANCIAL YEAR (From 15.11.2021 to 31.03.2022)

1.	Title of the Project/Scheme	Use of Thermal Autofrettage for Defence Applications
2.	Name of the Institution	Tezpur University
3.	Principal Investigator	Dr. Seikh Mustafa Kamal
4.	DRDO Letter No. and date of sanctioning the project Date of start of the project	ARMREB/ADMB/2021/234 14 June 2021 (Amendment dated 21 Sep 2021)
5.	Head of account as given in the original sanction letter	Major Head- NA Minor Head- NA
6.	Amount brought forward from the previous financial year quoting DRDO letter No. & date in which the authority to carry forward the said amount was given	Rs. 0.00
7.	Amount received during the financial year (Please give no. and date of DRDO sanction letter for the amount)	Rs. 24,96,682 ARMREB/ADMB/2021/234 dated 14 June 2021 (Amendment dated 21 Sep 2021)
8.	Amount of interest accrued, if any, from the grants	Rs. 20,852
9.	Total amount that was available for expenditure (excluding commitments) during the financial year (2021-2022) (SL. No 6+7+8)	Rs. 25,17,534
10.	Actual expenditure (excluding commitments) incurred during the financial year (2021- 2022)	Rs. 2,72,502
11.	Balance amount available at the end of the financial year	Rs. 22,45,032
12.	Unspent balance refunded, if any (Please give details of cheque No. etc.)	NIL
13.	Amount allowed to be carried forward to the next financial year	Rs. 22,45,032

UTILIZATION CERTIFICATE

FY (From 15.11.2021 to 31.03.2022)

Certified that sum of Rs. 41,33,726 was sanctioned as grants-in-aid during the year 2021-22 in favour of Registrar, Tezpur University (Instt) vide DRDO letter No/ ARMREB/ADMB/2021/234 & dated 14 June 2021 (Amendment dated 21 Sep 2021).

A sum of Rs. 24,96,682 released vide letter no. ARMREB/ADMB/2021/234 dated 14 June 2021 (Amendment dated 21 Sep 2021) an amount of Rs. 20,852 accrued as interest (if any) during the year and NIL on account of unspent balance of the previous year, a sum of Rs. 2,72,502 has been utilized for the purpose for which it was sanctioned and that the balance of Rs. 22,45,032 remaining unutilized at the end of the year will be adjusted toward the grants-in-aid payable during the next year i.e 2022-2023

31/7/2023

Principal Investigator

Accounts/Finance Officer
Finance Officer
Tezpur University

Administrative Authority
(with official seal)
Registrar
Tezpur University

2. Certified that I have satisfied myself that the conditions on which the grants-in-aid was sanctioned have been fulfilled/are being fulfilled and that I have exercised the following checks to see that the money was actually utilized for the purpose for which it was sanctioned.

Signature of Audit Authority of Grantee Institution

AUDITED/ PROVISIONAL STATEMENT OF EPENDITURE ACCOUNTS

For the Financial Year (1/4/2022 to 31/3/2023)

a. **Title of the Project**: Use of Thermal Autofrettage for Defence Application

b. **Sanctioned letter no. & date**: ARMREB/ADMB/2021/234 & 14 June 2021 (Amendment dated 21 Sep 2021)

c. **Principal Investigator**: Dr. Seikh Mustafa Kamal

d. **Date of start of the project**: 15 November, 2021

e. **Total sanctioned cost of the project in Rs**: Rs. 41,33,726/-

f. **Grant received (Rs.) in I yr** Rs. 24,96,682 **II yr** NIL **III yr** NIL

g. **Total grants received so far**: Rs. 24,96,682

S. No	Sanctioned Heads	Funds sanctioned for the year Rs.	Funds released Rs.	Carried forward from previous year Rs.	Funds available (iv+v) Rs.	Expenditure incurred during the FY Rs.	Balance (vi-vii) Rs.	Commitments Rs.	Total expenditure (vii+ix) Rs.
i	ii	iii	iv	v	vi	vii	viii	ix	x
(a)	Staff	4,31,520	NIL	3,89,207	3,89,207	2,92,392	96,815	NIL	2,92,392
(b)	Equipment	0	NIL	15,90,256	15,90,256	NIL	15,90,256	NIL	NIL
(c)	Operation & Maint.	NA	NA	NA	NA	NA	NA	NA	NA
(d)	Expendables	1,17,000	NIL	1,35,000	1,35,000	NIL	1,35,000	NIL	NIL
(e)	Travel	50,000	NIL	11,531	11,531	NIL	11,531	NIL	NIL
(f)	Contingencies	35,000	NIL	32,500	32,500	12,090	20,410	NIL	12,090
(g)	Research Consultant	NA	NA	NA	NA	NA	NA	NA	NA
(h)	Procured Service	NA	NA	NA	NA	NA	NA	NIL	NA
	Institutional over head	1,75,162	NIL	65,686	65,686	64,489	1,197	NIL	64,489
	Interest earned, if any			20,852	20,852+46,902		67,754		
	TOTAL	8,08,682	NIL	22,45,032	22,91,934	3,68,971	19,22,963	NIL	3,68,971

(Dr. SEIKH MUSTAFA KAMAL)
Name and Signature of
Principal Investigator
Date: 31/7/2023

Name and Signature of
Accounts Officer
04.8.23
Date:
Finance Officer
Tezpur University

Signature of Administrative
04/8/23
Date:
Registrar
Tezpur University

UTILIZATION CERTIFICATE

FOR THE FINANCIAL YEAR (From 1.04.2022 to 31.03.2023)

1.	Title of the Project/Scheme	Use of Thermal Autofrettage for Defence Applications
2.	Name of the Institution	Tezpur University
3.	Principal Investigator	Dr. Seikh Mustafa Kamal
4.	DRDO Letter No. and date of sanctioning the project Date of start of the project	ARMREB/ADMB/2021/234 14 June 2021 (Amendment dated 21 Sep 2021)
5.	Head of account as given in the original sanction letter	Major Head- NA Minor Head- NA
6.	Amount brought forward from the previous financial year quoting DRDO letter No. & date in which the authority to carry forward the said amount was given	Rs. 22,45,032
7.	Amount received during the financial year (Please give no. and date of DRDO sanction letter for the amount)	NIL
8.	Amount of interest accrued, if any, from the grants	Rs. 46,902
9.	Total amount that was available for expenditure (excluding commitments) during the financial year (2022-2023) (SL. No 6+7+8)	Rs. 22,91,934
10.	Actual expenditure (excluding commitments) incurred during the financial year (2022- 2023)	Rs. 3,68,971
11.	Balance amount available at the end of the financial year	Rs. 19,22,963
12.	Unspent balance refunded, if any (Please give details of cheque No. etc.)	Rs. 19,22,963
13.	Amount allowed to be carried forward to the next financial year	NIL

UTILIZATION CERTIFICATE

FY (From 1.04.2022 to 31.03.2023)

Certified that sum of Rs. 8,08,682 was sanctioned as grants-in-aid during the year 2022-23 infavour of Registrar, Tezpur University (Instt) vide DRDO letter No/ ARMREB/ADMB/2021/234 dated 14 June 2021 (Amendment dated 21 Sep 2021)

A sum of Rs. 0 released vide letter no. ARMREB/ADMB/2021/234 dated 14 June 2021 (Amendment dated 21 Sep 2021) an amount of Rs. 46,902 accrued as interest (if any) during the year and 22,45,032 on account of unspent balance of the previous year, a sum of Rs. 3,68,971 has been utilized for the purpose for which it was sanctioned and that the balance of Rs. 19,22,963 remaining unutilized at the end of the project will be refunded.

31/7/2023

Principal Investigator

Accounts/Finance Officer
Finance Officer
Tezpur University

Administrative Authority
(with official seal)
Registrar
Tezpur University

2. Certified that I have satisfied myself that the conditions on which the grants-in-aid was sanctioned have been fulfilled/are being fulfilled and that I have exercised the following checks to see that the money was actually utilized for the purpose for which it was sanctioned.

Signature of Audit Authority of Grantee Institution

ER/RB- 06

Form for Equipments Purchased

Assets acquired wholly for substantially out of government grants register maintained by grantee institution block account maintained by sanctioning authorities

Name of Sanctioning Authority: **Dte of ER & IPR, RBs** DRDO, Ministry of Defence, Government of India, New Delhi.

S. No.	Name of Grantee Institution	No. and date of sanction	Amount of sanctioned grant	Brief purpose of the grant	Whether any condition regarding the right of ownership of Govt. in the property or assets acquired out of the grant was incorporated in the grant-in-aid sanction	List of equipments as per approved proposal	Particulars of assets/equipments actually created or acquired
(1)	(2)	(3)	(4)	(5)	(6)	(7)	(8)
1.	Tezpur University	No.: ARMREB/ADMB/2021/234 Date of sanction: June 4, 2021 Amendment to sanction: Sept.14,2021 Sanction code: DGTM/TM/ARMREB/GIA/21-22/0148	Rs.41,33,726/-	To investigate the thermal autofrettage process in order to assess its feasibility for defence applications	No	i. Strain gauge DAQ module & installation kit ii. Thermocouple welder iii. Induction heating machine iv. Centrifugal pump v. Workstation	Workstation DT DELL OPTIPLEX 5080 Core i5/16 GB/1 TB +256 SSD

Contd...

Value of the assets as on ……(date of submission)	Purpose for which utilized at present	Encumbered or not	Reason if encumbered	Disposed of or not	Reasons & authority if any, for disposal	Amount realized on disposal	Remarks
(9)	(10)	(11)	(12)	(13)	(14)	(15)	(16)
Rs. 79,744/-	For computational modeling of thermal autofrettage system	NA	NA	NA	NA	NA	

20/7/2023

(Principal Investigator)

04.8.23

Accounts Officer

Finance Officer
Tezpur University

04/8/23

Administrative Authority

Registrar
Tezpur University

ER/RB-08

Retaining Facilities created/ Equipment procured form

(Assets acquired out of government grants to be retained by grantee institution)

Name of Sanctioning Authority: Dte of ER & IPR, RBs DRDO, Ministry of Defence, Government of India, New Delhi

Ref: (Use of Thermal Autofrettage for Defence Application, ARMREB/ADMB/2021/234, dated June 4, 2021, Amendment dated Sep 21, 2021)

Particulars of Facility created/ Equipment Procured	Workstation : DT DELL OPTIPLEX 5080 Corei5/16 GB/1 TB+256 SSD
Value of the asset	Rs. 79,744/-
S.No. of Equipment in ER-06 list of the Project	(v)
Name of PI	Dr. Seikh Mustafa Kamal
Contact Details (Email, Phone, Fax, mobile No.)	smkmech@tezu.ernet.in, 08473894159
Name and address of Grantee Institution	Tezpur University
No. and date of sanction	No.: ARMREB/ADMB/2021/234, Date: June 4, 2021, Amendment dated Sep 21, 2021.
Amount of sanctioned grant	Rs. 41,33,726
Purpose for which utilized	For Numerical Simulation
Justification for retaining assets created or acquired	The asset is required for numerical works to be carried out for the proposed extended works on thermal autofrettage (which is ready for submission to ADMB panel, ARMREB as per the suggestion of the last panel meeting held on March 25, 2023, which is also stated in the MoM). Further, the asset will be utilized for the numerical works of M.Tech and PhD students of the department.

20/7/2023
(Principal Investigator)

04.8.23
(Accounts Officer)
Finance Officer
Tezpur University

(Administrative Authority)
Registrar
Tezpur University

TEZPUR UNIVERSITY
(A Central University Established by an Act of Parliament)
NAPAAM, TEZPUR – 784028
DISTRICT: SONITPUR:: ASSAM:: INDIA

July 20, 2023

To

The Secretary, ARMREB

Subject: Request for the retention of the equipment purchased.

Ref. Project: Use of Thermal Autofrettage for Defence Application,
No. ARMREB/ADMB/2021/234, Dated 4 June 2021, Amended on 21 Sep 2021.

Sir,

The following equipment was purchased under the above referred project with the details below:

Sr. No	Description	Equipment	Date	Details of Cost
1.	Workstation	DT DELL OPTIPLEX 5080 Core i5/16 GB/1 TB +256 SSD	25.03.2022	Rs. 79,744/-

This is to request your kind permission to retain the equipment for in house R&D/ new project proposal.

Upon retention of the same, we undertake that

- Equipment will be made available to DRDO for use without any payment.
- Expenditure incurred for maintenance/ up keep of the same will be borne by the University.
- Permission will be taken from ARMREB/DRDO HQ before disposal of the same.
- Salvage value of the equipment store to be reimbursed to DRDO/ARMREB within one month through MRO/DRAFT of the disposal.

20/7/2023
Principal Investigator

Kalita 20/07/2023
Head
Dept. of Mechanical Engg
Tezpur University
Head of the Department

Finance Officer
Tezpur University
Finance Officer

Assets Retaining Requistion form

DRDO grant of Rs. 41,33,726/- (Rs. Fourty one lac thirty three thousand seven hundred twenty six) sanctioned vide letter No. ARMREB/ADMB/2021/234 dated 4 June 2021, amended on Sep 21, 2021, received for project on the subject/topic use of thermal autofrettage for defence application for a period of 03 years.

Permission is being sought to retain the Assets procured under the grant-in-aid project. Particulars are mentioned in the 'Retaining Facilities created/Equipment procured Form' attached herewith.

20/7/2023
(Dr. SEIKH MUSTAFA KAMAL)

(Signature & Name of PI)

(Signature & Name of Administrative Authority)

Registrar
Tezpur University

List of equipment purchased under the project along with details of cost, source date of purchase, name and name of inventory holder

Sanctioned Special Equipment

1. Workstation (for numerical analysis)

Sr. No	Description	Equipment	Date	Details of Cost
1.	Workstation	DT DELL OPTIPLEX 5080 Core i5/16 GB/1 TB +256 SSD	25.03.2022	Rs. 79,744/-

31/7/2023

(Principal Investigator)

31/8/2023

Accounts Officer

Finance Officer

Tezpur University

01/9/23

Administrative

Registrar

Tezpur University